Reservoir scale numerical simulation of CO_2 injection into Lower Tuscaloosa Formation in Mississippi, USA with experimentally validated modeling parameters

Liwei Zhang, Yee Soong, Robert Dilmore

National Energy Technology Laboratory (NETL), U. S. DOE

NATIONAL ENERGY TECHNOLOGY LABORATORY

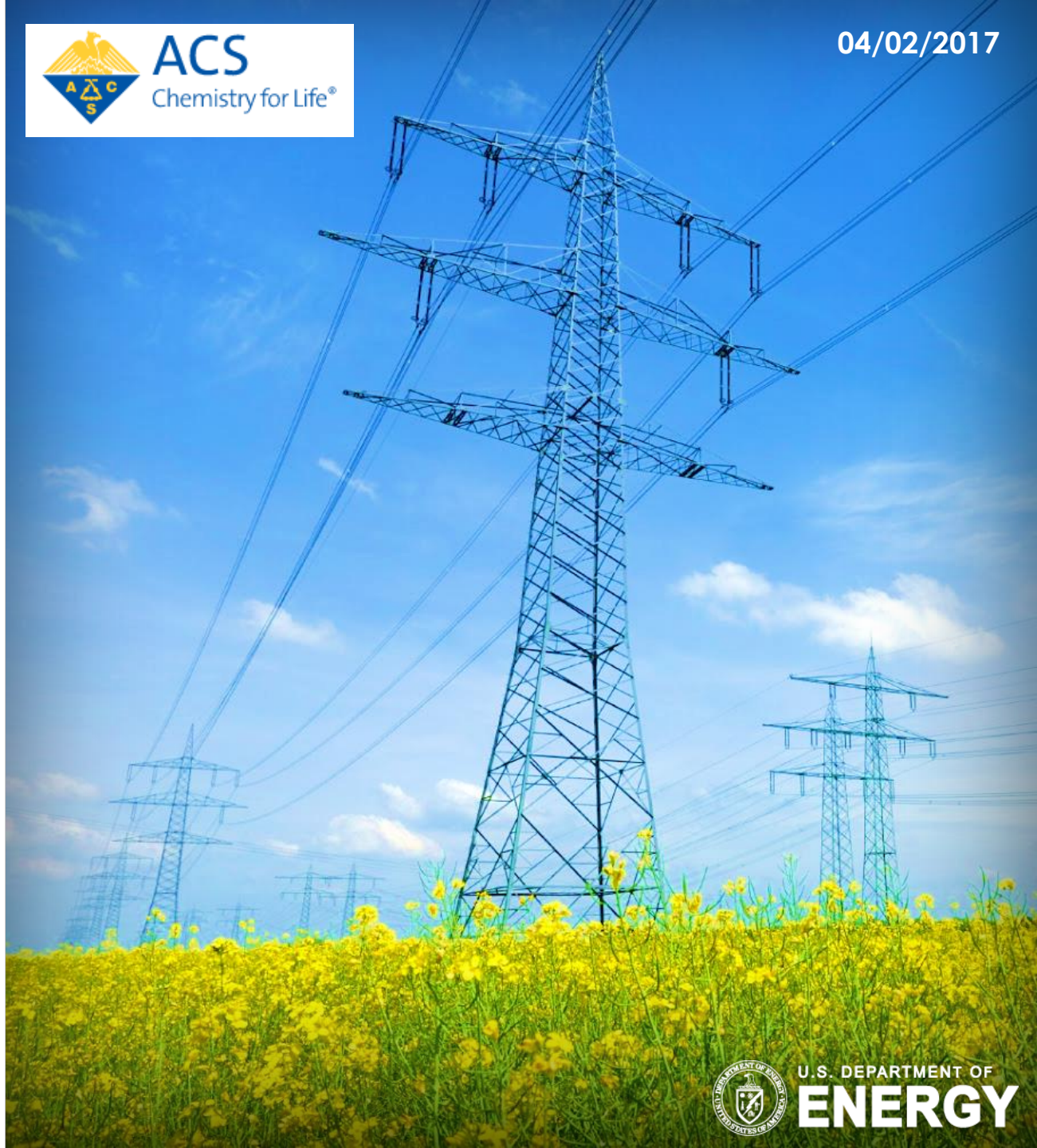

Acknowledgments

This research was supported in part by an appointment to the National Energy Technology Laboratory Research Participation Program, sponsored by the U.S. Department of Energy and administered by the Oak Ridge Institute for Science and Education.

The authors would like to thank the Research and Innovation Center (RIC) at NETL for funding support and providing access to research article databases. The authors also would like to thank Dustin Crandall at NETL Morgantown site and Bret Howard at NETL Pittsburgh site for CT, SEM and XRD analyses on rock samples used in this study.

Contents

Introduction

Carbon Capture, Utilization and Sequestration (CCUS)

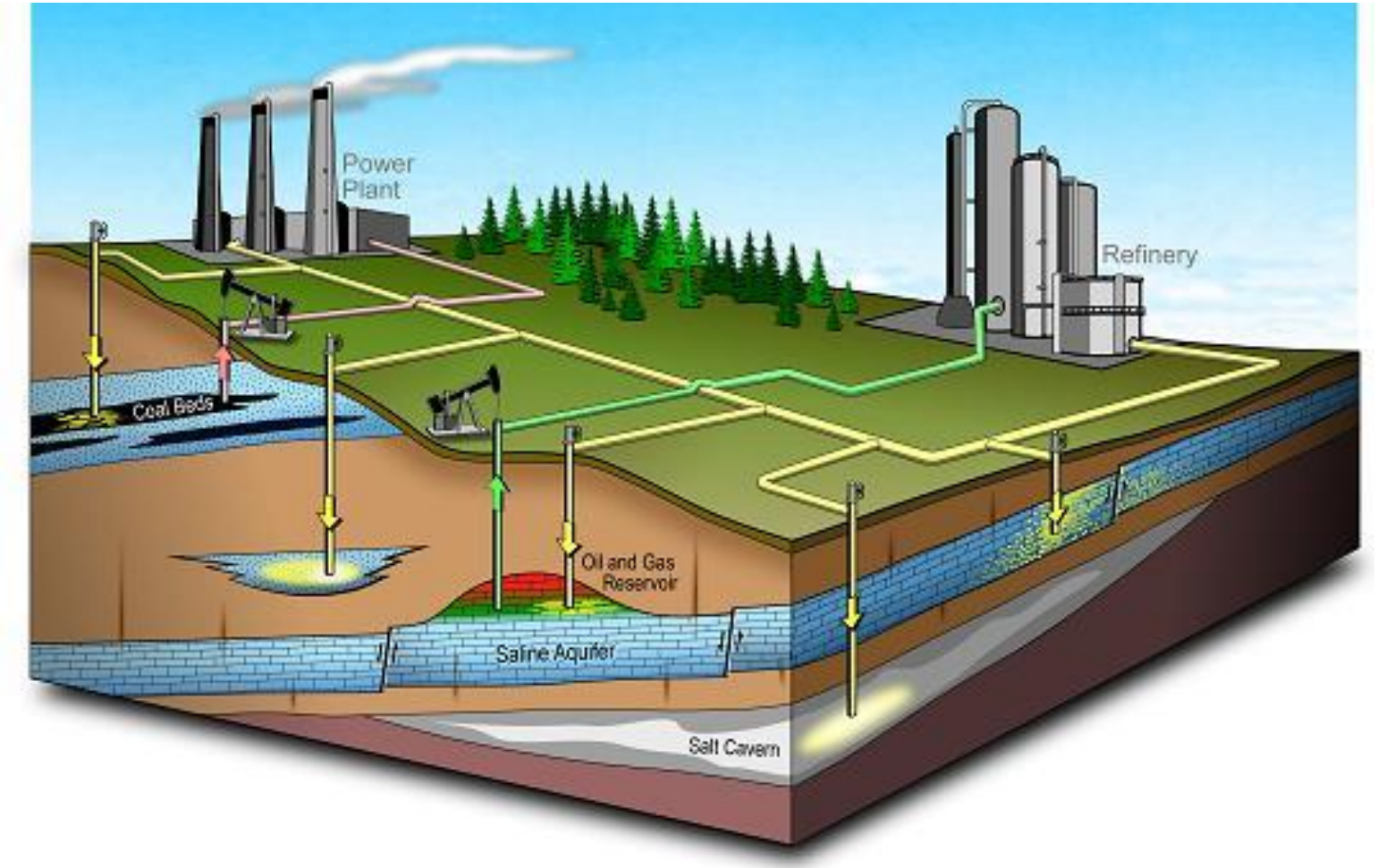

Introduction

Geologic Sink Capacity Estimates--*Adequate Storage Projected*

U.S. emissions ~ 6 Gt CO_2 / yr, all sources

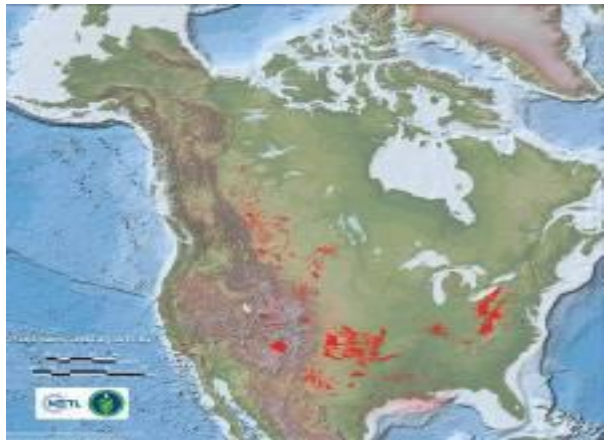

Oil and Gas Fields

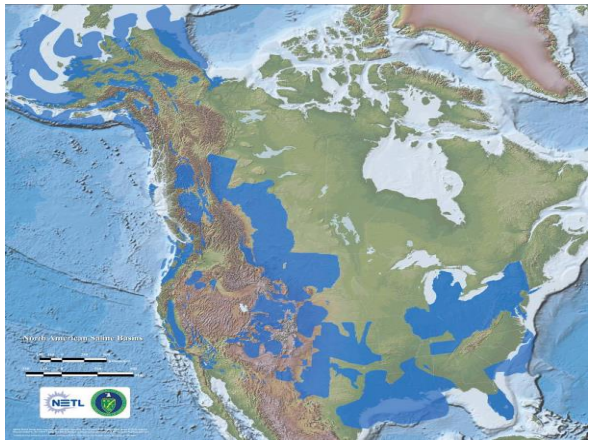

Saline Formations

4,674 stationary sources identified

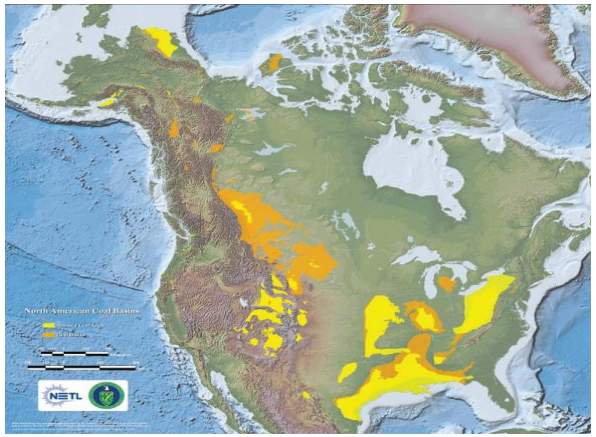

Unmineable Coal Seams

Conservative resource assessment

Estimated North American CO_2 Storage Potential (Gigatonnes)

Sink Type	Low	High
Oil and Gas Fields	140	140
Saline Formations	3,300	12,600
Unmineable Coal Seams	160	180

Hundreds of years storage potential

Introduction

- CO_2 storage reservoir: Lower Tuscaloosa Sandstone Formation; caprock: Marine Shale Formation (Southeast Regional Carbon Sequestration Partnership Project).
- Two rock samples (one from the reservoir and one from the caprock) were obtained.
- Both samples were exposed to CO_2-saturated brine under a pressure of 23.8 MPa and a temperature of 85°C for 180 days.
- Laboratory-conducted permeability measurements show permeability changes of the samples after 180 days of exposure to CO_2-saturated brine.
- A small-scale reactive transport model is developed and results from the model demonstrate key mineral precipitation and dissolution processes that cause permeability changes of the samples.

Introduction

Experimental studies (Soong et al., 2016, 2017)

High-pressure vessel

Core sample

Permeability measurement

Two samples are tested: one Lower Tuscaloosa Formation sample and one Marine Shale Caprock sample

Introduction

Results of experimental studies

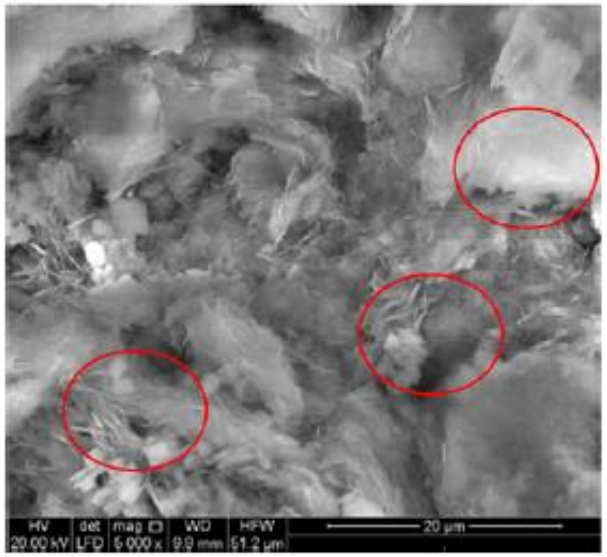

Fresh Lower Tuscaloosa sample

Dissolution of silicates

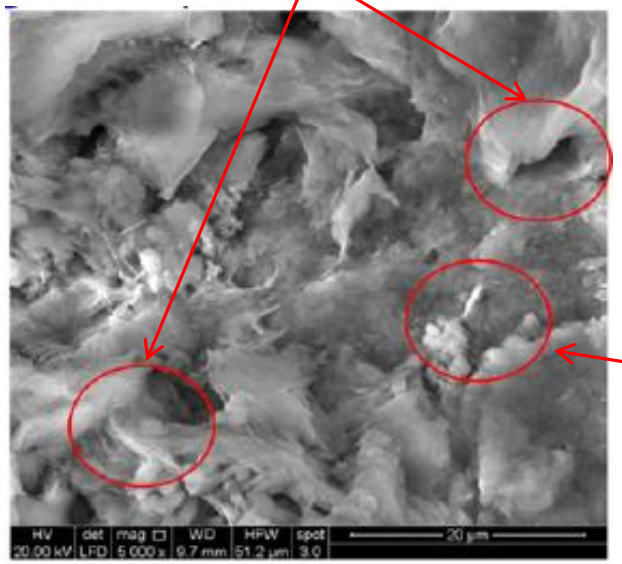

Exposed Lower Tuscaloosa sample

Possible precipitation of SiO_2 (am), kaolinite and barite

	LT	LT after 6 months	Marine Shale	Marine Shale after 6 months
Porosity	26.8%	25.0%	8.65%	8.56%
Permeability	2190 mD	1925 mD	47 uD	192 uD

Introduction

Mineral compositions and porosity of unreacted Lower Tuscaloosa sandstone

Sample taken from 2603 m depth at Lower Tuscaloosa Formation, Jackson County, Mississippi

Mineral name	Volume percentage (%, before reaction with brine and CO_2)	Specific surface area (m^2/g)	Molar volume (cm^3/mol)
Mineral compositions of unreacted Lower Tuscaloosa sandstone			
Chlorite $(Mg_{2.964}Fe_{1.927}Al_{2.483}Ca_{0.011}Si_{2.633}O_{10}(OH)_8)$	1.46	5.06	210.3
Microcline ($KAlSi_3O_8$)	0.73	0.39	100.4
Muscovite/Illite $(K_{0.85}Al_{2.85}Si_{3.15}O_{10}(OH)_2)$	0.73	3.40	144.5
Kaolinite $(Al_2Si_2O_5(OH)_4)$	0.73	15.0	99.3
Na-feldspar $(NaAlSi_3O_8)$	1.46	0.39	100.4
Quartz (SiO_2)	67.3	0.10	22.7
Calcite ($CaCO_3$)	0.79	1.00	36.9
Porosity	26.8	--	--

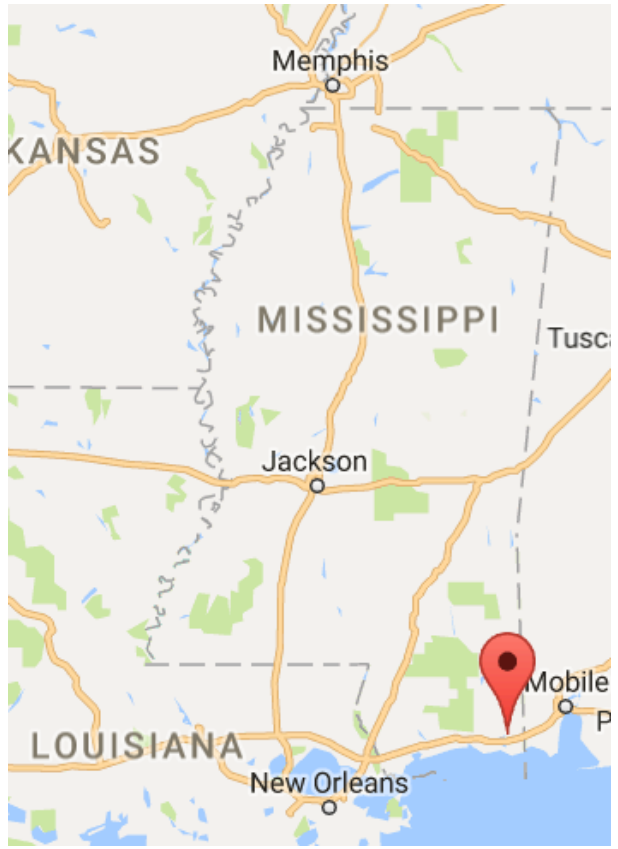

Introduction

Mineral compositions and porosity of unreacted Marine Shale caprock

Sample taken from 2418 m depth at Marine Shale Formation, Jackson County, Mississippi

Mineral name	Volume percentage (%, before reaction with brine and CO_2)	Specific surface area (m^2/g)	Molar volume (cm^3/mol)
Mineral compositions of unreacted Marine Shale caprock			
Chlorite ($Mg_{2.964}Fe_{1.927}Al_{2.483}Ca_{0.011}Si_{2.633}O_{10}(OH)_8$)	8.22	0.30	210.3
Microcline ($KAlSi_3O_8$)	1.83	0.39	100.4
Muscovite/Illite ($K_{0.85}Al_{2.85}Si_{3.15}O_{10}(OH)_2$)	4.57	5E-4	144.5
Kaolinite ($Al_2Si_2O_5(OH)_4$)	4.57	15.0	99.3
Na-feldspar ($NaAlSi_3O_8$)	5.48	0.39	100.4
Quartz (SiO_2)	54.8	0.10	22.7
Calcite ($CaCO_3$)	4.57	1.00	36.9
Ca-feldspar ($CaAl_2Si_2O_8$)	5.48	0.39	101.9
Inert mineral	1.83	--	--
Porosity	8.65	--	--

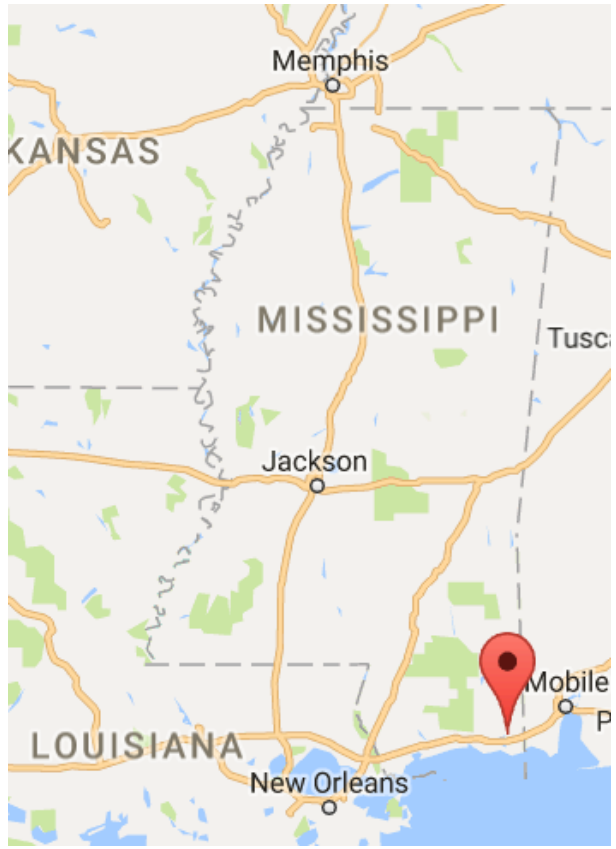

Core-scale model

Model domain and governing equations

1-D no flow reactive transport model

Software used: CrunchFlow

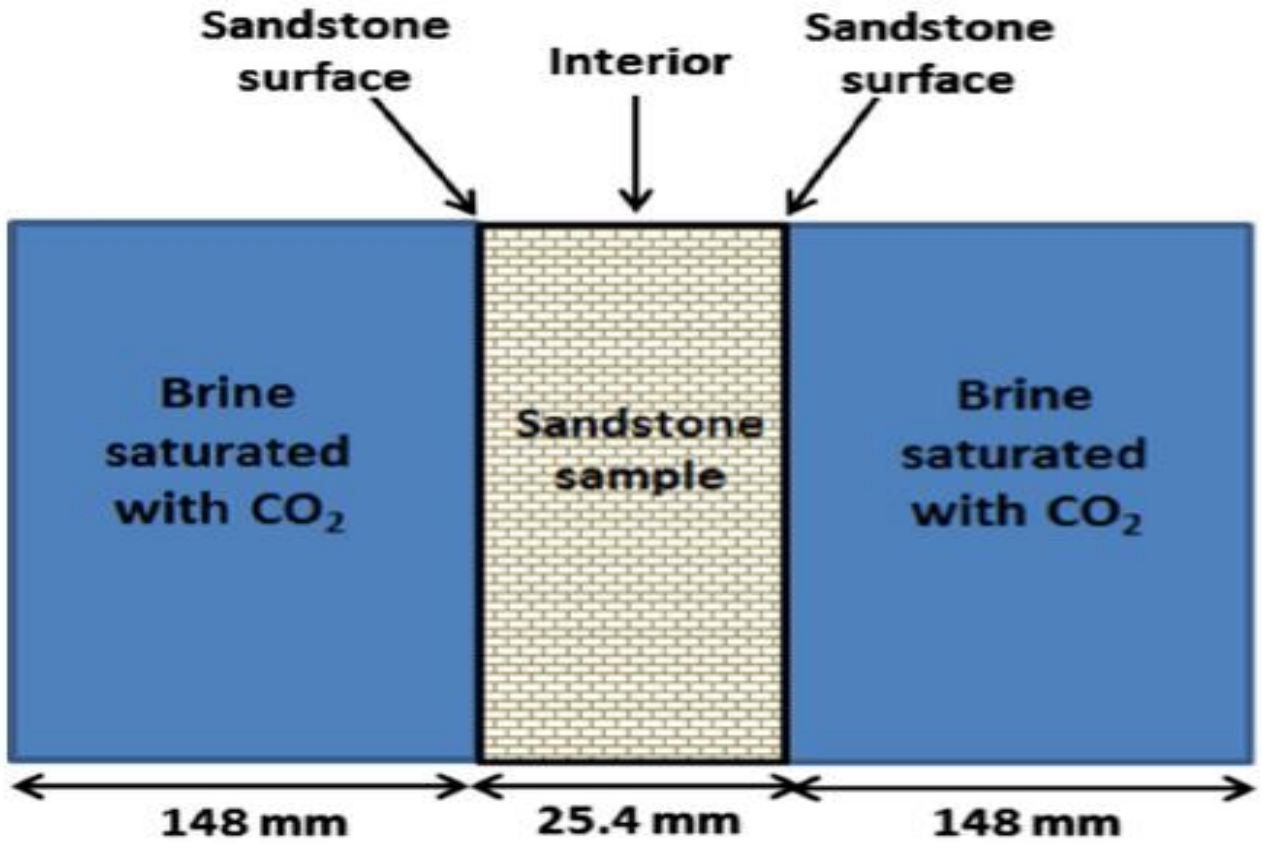

Mass conservation equation

$$\frac{d(\phi C_i)}{dt} = \frac{d}{dx}(\phi D_{ie}\frac{dC_i}{dx}) \pm \sum_{i=1}^{N} v_{ir}R_{ir}$$

Diffusion term Reaction term

Porosity evolution equation

$$\phi(t) = 1 - \sum_{i=1}^{m} fr_i(t) - fr_n$$

Rate of mineral dissolution/precipitation

$$R_{ir} = A\sum_{l=1}^{M} k_l \left(\prod_{i=1}^{N} a_i^{p_i}\right)\left(1 - \frac{Q}{K_{eq}}\right)$$

Effective diffusivity

$$D_e = D_0\phi^m$$

Core-scale model

Equilibrium constants (K_{eq}) and reaction rate constants (k)

Reaction	Equilibrium Constant at 85°C (K_{eq})	Rate Coefficient at 85°C, k, mol/(m²s)	Value of $\prod_{i=1}^{N} a_i^{p_i}$
Calcite dissolution/precipitation (85 °C) $CaCO_3 + H^+ \leftrightarrow Ca^{2+} + HCO_3^-$	$10^{0.996}$ (BRGM)	For dissolution, $k_1 = 10^{-2.01}$; for precipitation, $k_2 = 10^{-7.31}$ (Zhang et al.)	For dissolution, $\prod_{i=1}^{N} a_i^{p_i} = a_{H^+}$; for precipitation, $\prod_{i=1}^{N} a_i^{p_i} = a_{Ca2+} \times a_{HCO3-}$ (Zhang et al.)
Chlorite dissolution (85 °C) $Mg_{2.964}Fe_{1.927}Al_{2.483}Ca_{0.011}Si_{2.633}O_{10}(OH)_8) + 17.468H^+ \leftrightarrow K^+ + 2.483Al^{3+} + 0.011Ca^{2+} + 1.712Fe^{2+} + 2.964Mg^{2+} + 2.633H_4SiO_4(aq) + 0.215Fe^{3+} + 7.468H_2O$	$10^{42.37}$ (BRGM)	$10^{-9.17}$ (calculated from k at 25 °C in Smith et al.)	The dissolution is pH-dependent. $\prod_{i=1}^{N} a_i^{p_i} = a_{H^+}{}^{0.49}$ (Smith et al.)
Dolomite dissolution/precipitation (85 °C) $CaMg(CO_3)_2 + 2H^+ \leftrightarrow Ca^{2+} + Mg^{2+} + 2HCO_3^-$	$10^{1.425}$ (Zhang et al.)	$10^{-14.43}$ (Zhang et al.)	1.0
$Fe(OH)_3$ dissolution/precipitation (85 °C) $Fe(OH)_3 + 3H^+ \leftrightarrow Fe^{3+} + 3H_2O$	$10^{0.99}$ (BRGM)	$10^{-7.46}$ (calculated from k at 25 °C in Brantley et al., given an activation energy of 62.8 kJ/mol in Wolery)	1.0
$Fe(OH)_2$ dissolution/precipitation (85 °C) $Fe(OH)_2 + 2H^+ \leftrightarrow Fe^{2+} + 2H_2O$	$10^{10.33}$ (BRGM)	$10^{-7.46}$ (assumed to be the same as that of $Fe(OH)_3$)	1.0

$$R_{ir} = A \sum_{l=1}^{M} k_l \left(\prod_{i=1}^{N} a_i^{p_i} \right) \left(1 - \frac{Q}{K_{eq}} \right)$$

Core-scale model

Gypsum dissolution/precipitation (85 °C) $CaSO_4 \cdot 2H_2O \leftrightarrow Ca^{2+} + SO_4^{2-} + 2H_2O$	$10^{-4.885}$ (Zhang et al.)	$10^{-4.16}$ (Zhang et al.)	1.0
Kaolinite dissolution/precipitation (85 °C) $Al_2Si_2O_5(OH)_4 + 6H^+ \leftrightarrow 2Al^{3+} + H_2O + 2H_4SiO_4(aq)$	$10^{1.56}$ (Zhang et al.)	For dissolution, $k_1=10^{-10.10}$; for precipitation, $k_2 = 10^{-12.15}$ (Zhang et al.)	For dissolution, $\prod_{i=1}^{N} a_i^{p_i} = a_{H^+}^{0.4}$; for precipitation, $\prod_{i=1}^{N} a_i^{p_i} = 1.0$
Microcline dissolution/precipitation (85 °C) $KAlSi_3O_8 + 4H^+ + 4H_2O \leftrightarrow K^+ + Al^{3+} + 3H_4SiO_4(aq)$	$10^{-1.58}$ (Zhang et al.)	For pH-independent dissolution/ precipitation, $k_1 = 10^{-11.29}$; For pH-dependent dissolution, $k_2 = 10^{-8.54}$	For pH-independent dissolution/ precipitation, $\prod_{i=1}^{N} a_i^{p_i} = 1.0$; For pH-dependent dissolution,
Montmorillonite dissolution/precipitation (85 °C) $Mg_{0.34}Al_{1.66}Ca_{0.17}Si_4O_{10}(OH)_2 + 6H^+ + 4H_2O \leftrightarrow 1.66Al^{3+} + 0.17Ca^{2+} + 0.34Mg^{2+} + 4H_4SiO_4(aq)$	$10^{-0.2}$ (BRGM)	For pH-independent dissolution/ precipitation, $k_1 = 10^{-10.96}$; For pH-dependent dissolution, $k_2 = 10^{-10.52}$ (Carroll et al.)	For pH-independent dissolution/ precipitation, $\prod_{i=1}^{N} a_i^{p_i} = 1.0$; For pH-dependent dissolution, $\prod_{i=1}^{N} a_i^{p_i} = a_{H^+}^{0.3}$ (Carroll et al.)
Muscovite/illite dissolution/precipitation (85 °C) $K_{0.85}Al_{2.85}Si_{3.15}O_{10}(OH)_2 + 10H^+ \leftrightarrow 3Al^{3+} + K^+ + 3H_4SiO_4(aq)$	$10^{4.03}$ (BRGM)	For pH-independent dissolution/ precipitation, $k_1 = 10^{-10.33}$ (Zhang et al.) For pH-dependent dissolution, $k_2 = 10^{-10.54}$ (derived from 25°C value in Bibi et al.)	For pH-independent dissolution/ precipitation, $\prod_{i=1}^{N} a_i^{p_i} = 1.0$; For pH-dependent dissolution, $\prod_{i=1}^{N} a_i^{p_i} = a_{H^+}^{0.37}$ (Bibi et al.)

Na-rich feldspar dissolution/precipitation (85 °C) $NaAlSi_3O_8 + 4H^+ + 4H_2O \leftrightarrow Na^+ + Al^{3+} + 3H_4SiO_4(aq)$	$10^{-0.64}$ (Zhang et al.)	For pH-independent dissolution/ precipitation, $k_1 = 10^{-11.29}$; For pH-dependent dissolution, $k_2 = 10^{-8.54}$ (Carroll et al.)	For pH-independent dissolution/ precipitation, $\prod_{i=1}^{N} a_i^{p_i} = 1.0$; For pH-dependent dissolution, $\prod_{i=1}^{N} a_i^{p_i} = a_{H^+}{}^{0.5}$ (Carroll et al.)
Quartz dissolution/precipitation (85 °C) $SiO_2 + 2H_2O \leftrightarrow H_4SiO_4(aq)$	$10^{-2.94}$ (BRGM)	$10^{-11.38}$ (Zhang et al.)	1.0
SiO_2 (am) dissolution/precipitation (85 °C) $SiO_2(am) + 2H_2O \leftrightarrow H_4SiO_4(aq)$	$10^{-3.00}$ (using chalcedony data from Wolery)	$10^{-6.47}$ (modified from $10^{-7.09}$ in Zhang et al. to fit solution chemistry data)	1.0
Siderite dissolution/precipitation (85 °C) $FeCO_3 + H^+ \leftrightarrow Fe^{2+} + HCO_3^-$	$10^{-1.20}$ (BRGM)	8.76×10^{-12} (Xu et al.)	For pH-independent dissolution/ precipitation, $\prod_{i=1}^{N} a_i^{p_i} = 1.0$; For pH-dependent dissolution, $\prod_{i=1}^{N} a_i^{p_i} = a_{H^+}{}^{0.9}$

Core-scale model--results

Porosity change—Lower Tuscaloosa

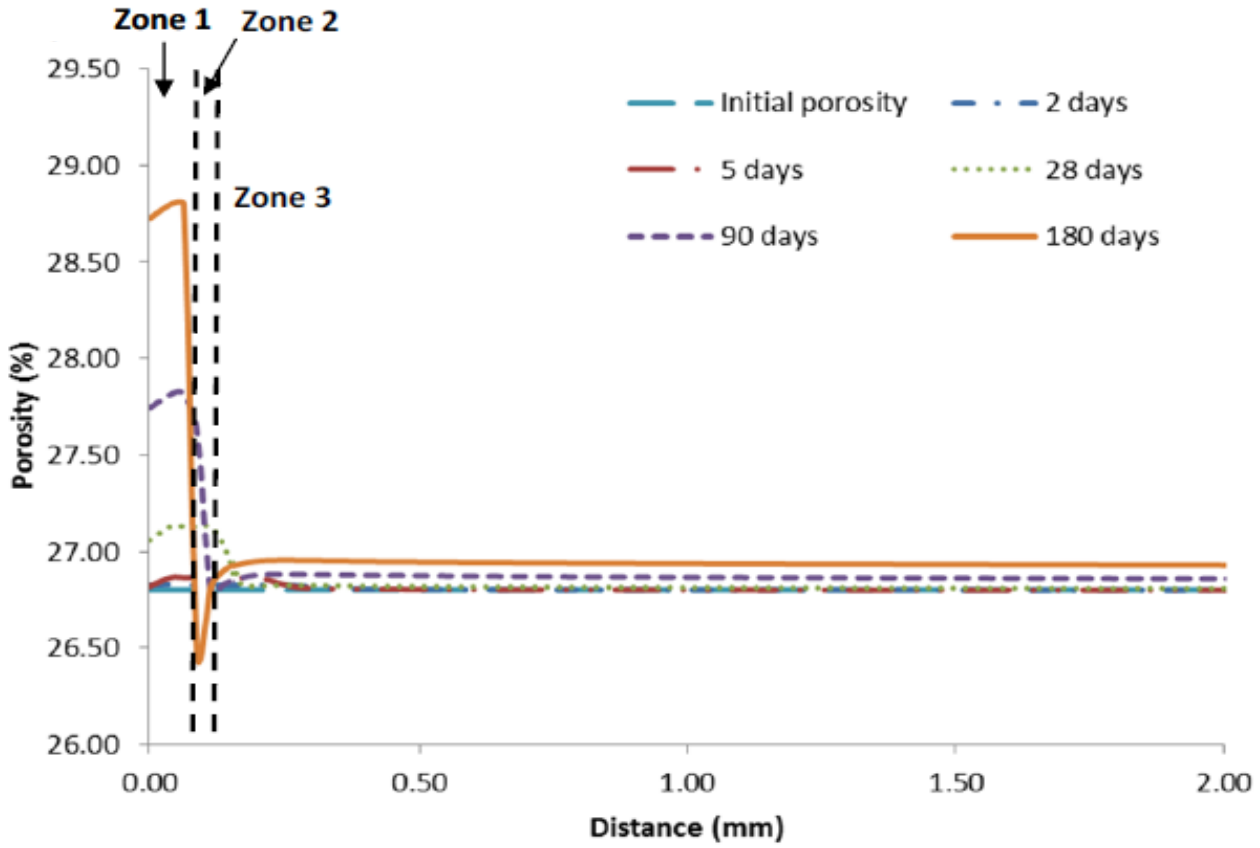

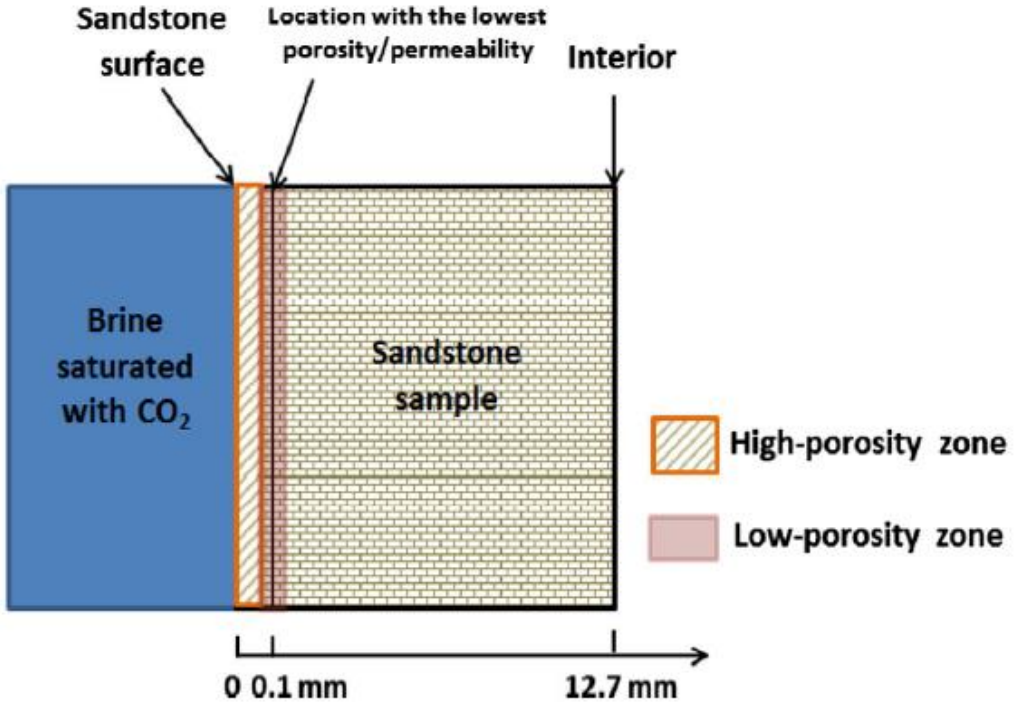

Core-scale model--results

Mineral composition change—Lower Tuscaloosa

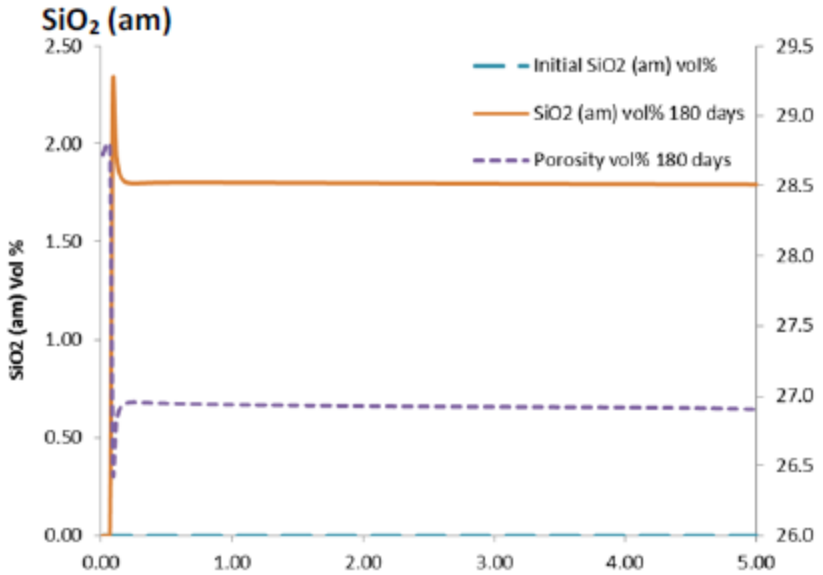

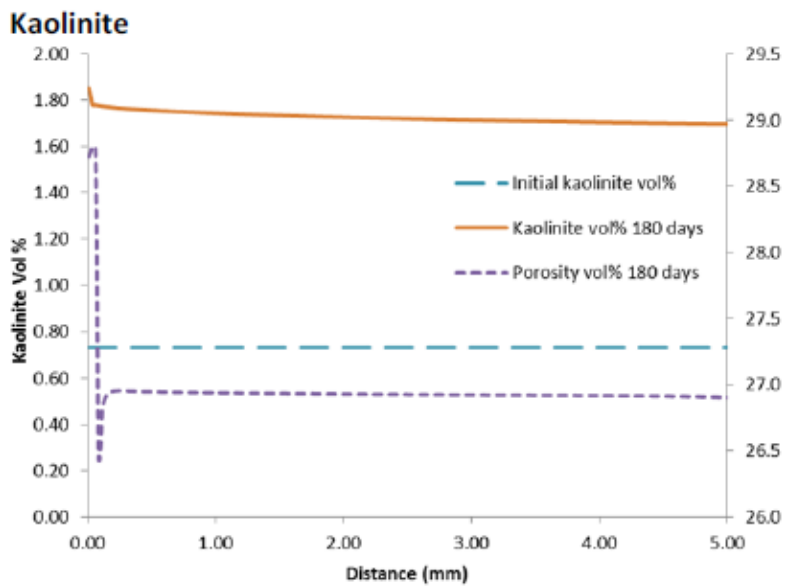

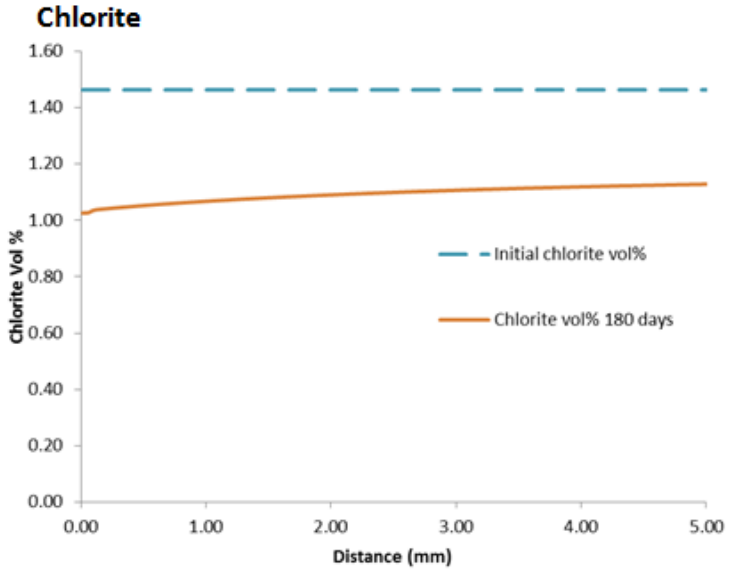

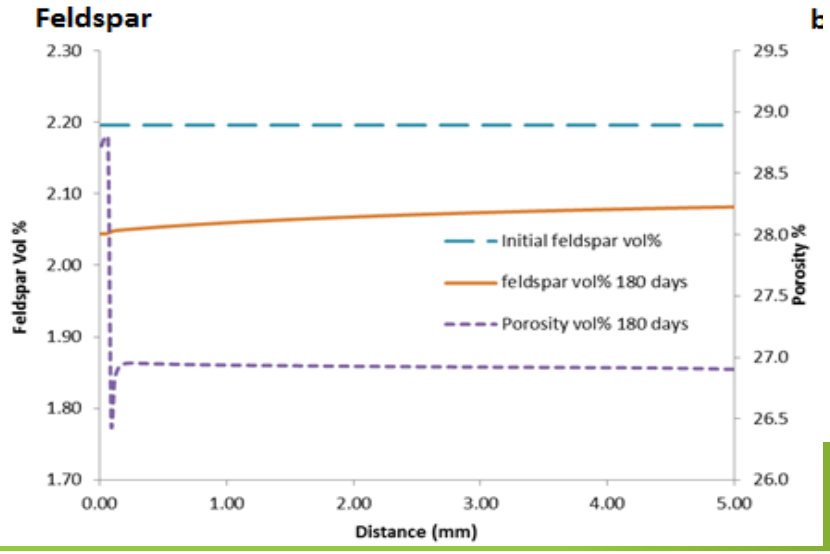

Core-scale model--results

Permeability calculation

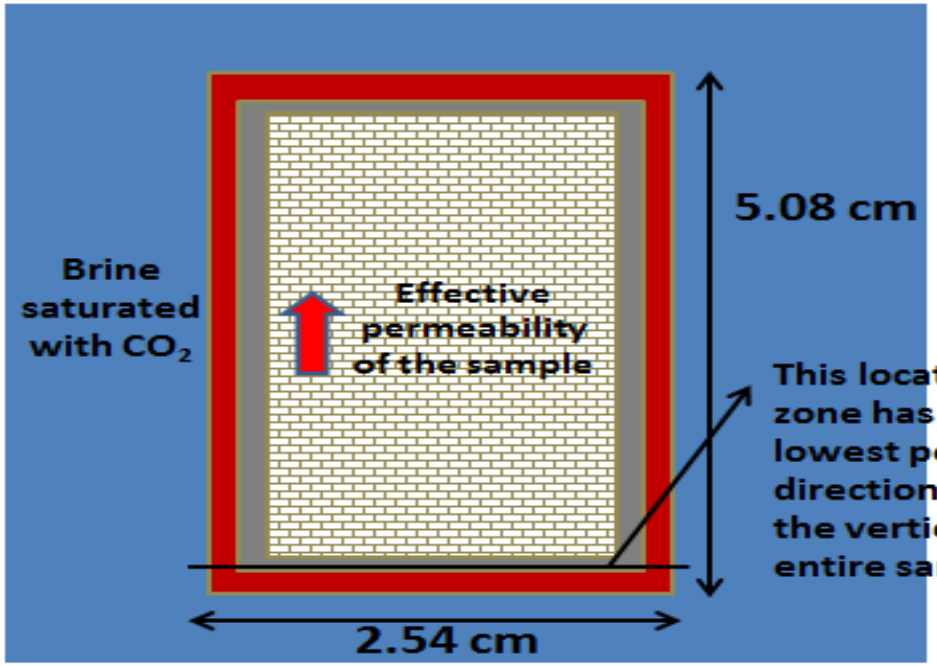

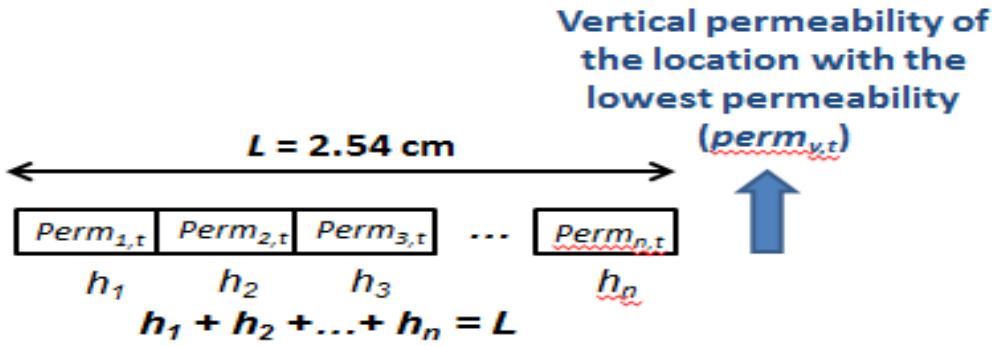

$$perm_{v,t} = \frac{\sum_{i=1}^{n} h_i perm_{i,t}}{L}$$

Calculation of $perm_{i,t}$ (Kumpel, 2003):

$$\frac{perm_{i,t}}{perm_{i,0}} = \left(\frac{\emptyset_{i,t}}{\emptyset_{i,0}}\right)^{n}$$

Core-scale model--results

Solution chemistry and permeability change—180 days (Lower Tuscaloosa)

Element/ component	Lower Tuscaloosa	
	Measured concentration (mg/kg water)	Model-predicted concentration (mg/kg water)
Ca	13,201	11,829
Na	48,387	43,946
Mg	1,240	1,130
K	530.0	576.8
Fe	210.0	137.9
Si	22.90	9.743
Al	2.200	97.77
Ba	5.900	0.160
Dissolved CO_2	Not measured	29,546

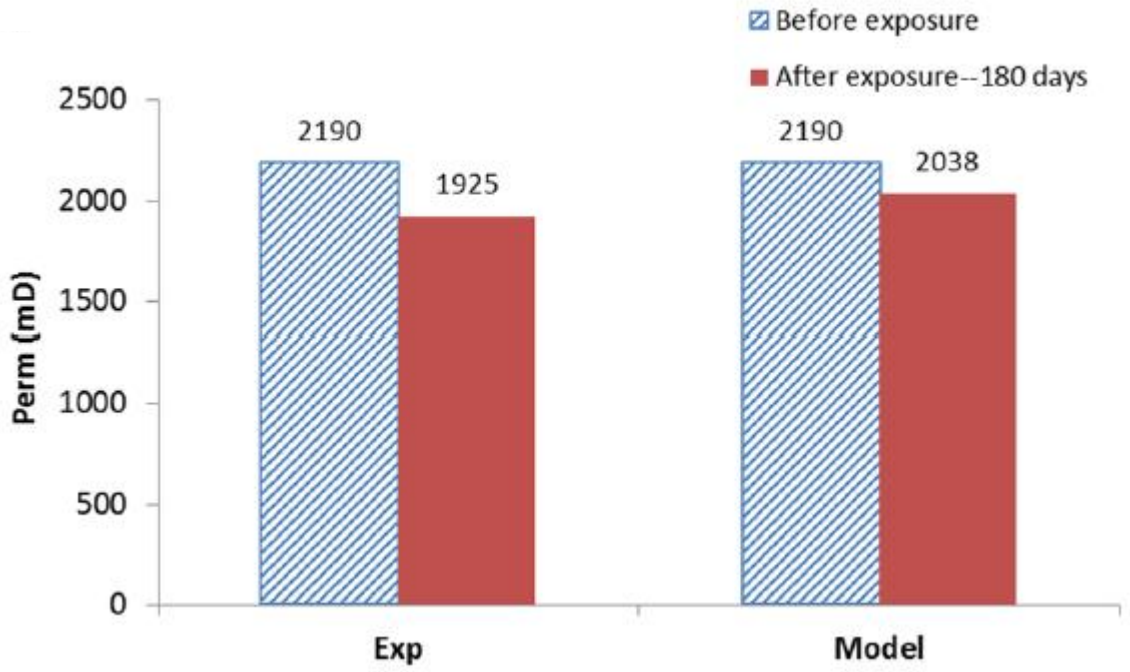

$$\frac{perm_{i,t}}{perm_{i,o}} = \left(\frac{\emptyset_{i,t}}{\emptyset_{i,o}}\right)^{6.0}$$

Core-scale model--results

Porosity change—Marine Shale

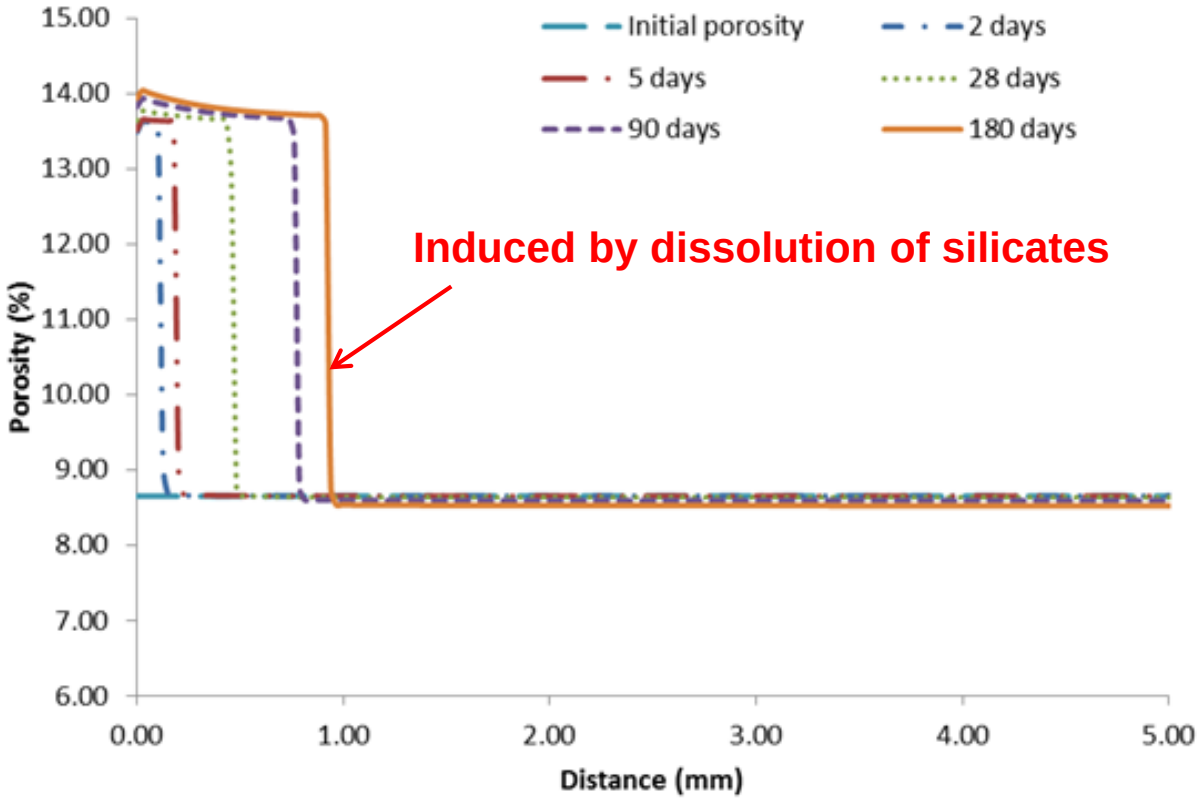

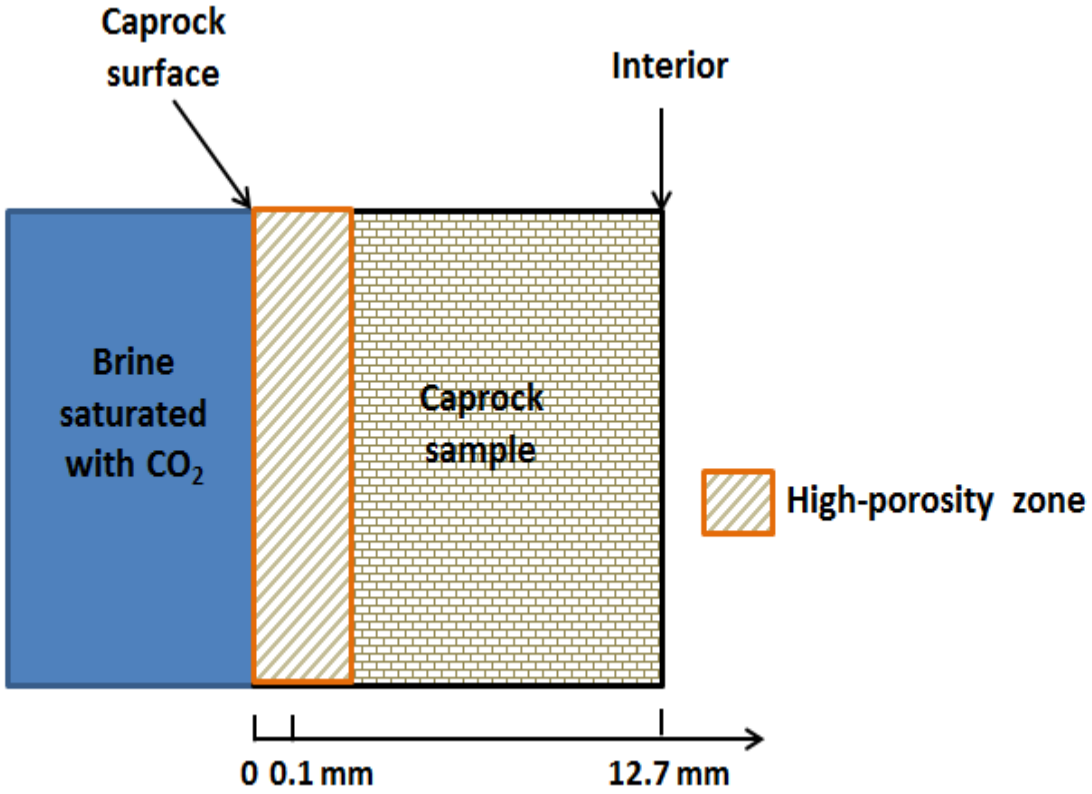

Core-scale model--results

Solution chemistry and permeability change—180 days (Marine Shale)

Element/ component	Marine Shale	
	Measured concentration (mg/kg water)	Model-predicted concentration (mg/kg water)
Ca	11,392	11,628
Na	43,073	42,168
Mg	1,081	1,087
K	340.0	330.5
Fe	205.0	232.4
Si	35.0	18.2
Sr	565.0	347.0
Ba	2.0	0.3
Dissolved CO_2	Not measured	30,369

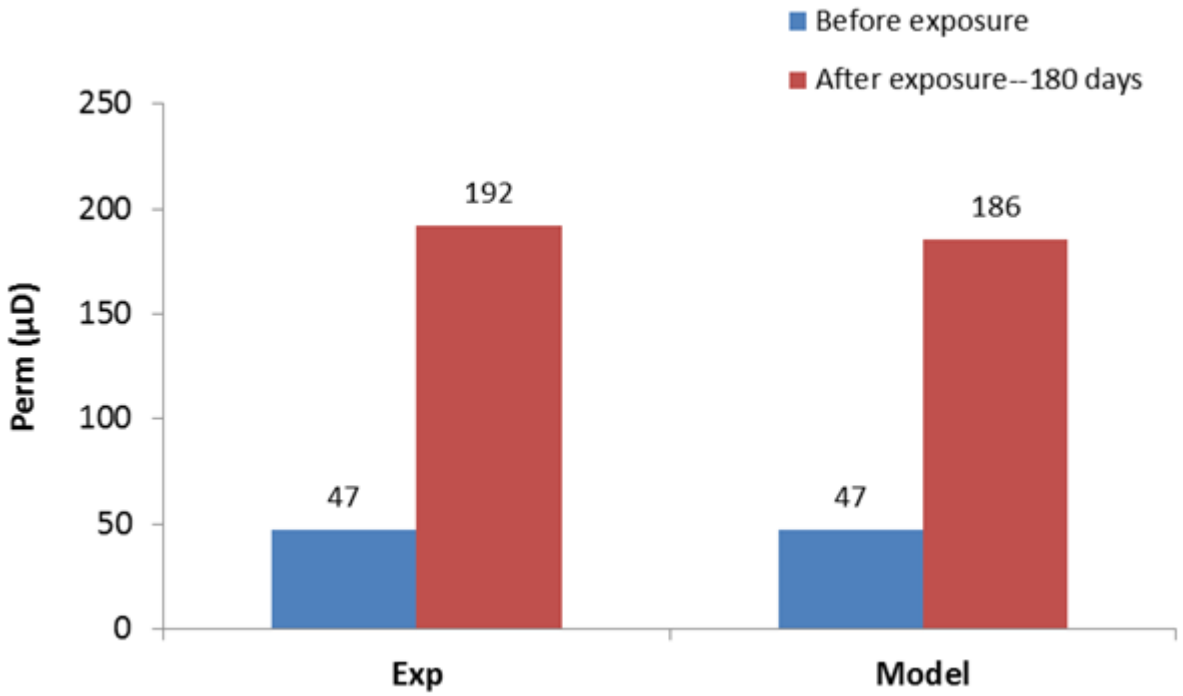

$$\frac{perm_{i,t}}{perm_{i,0}} = \left(\frac{\emptyset_{i,t}}{\emptyset_{i,0}}\right)^{8}$$

Discussion

Potential over-prediction of permeability increase for Marine Shale sample

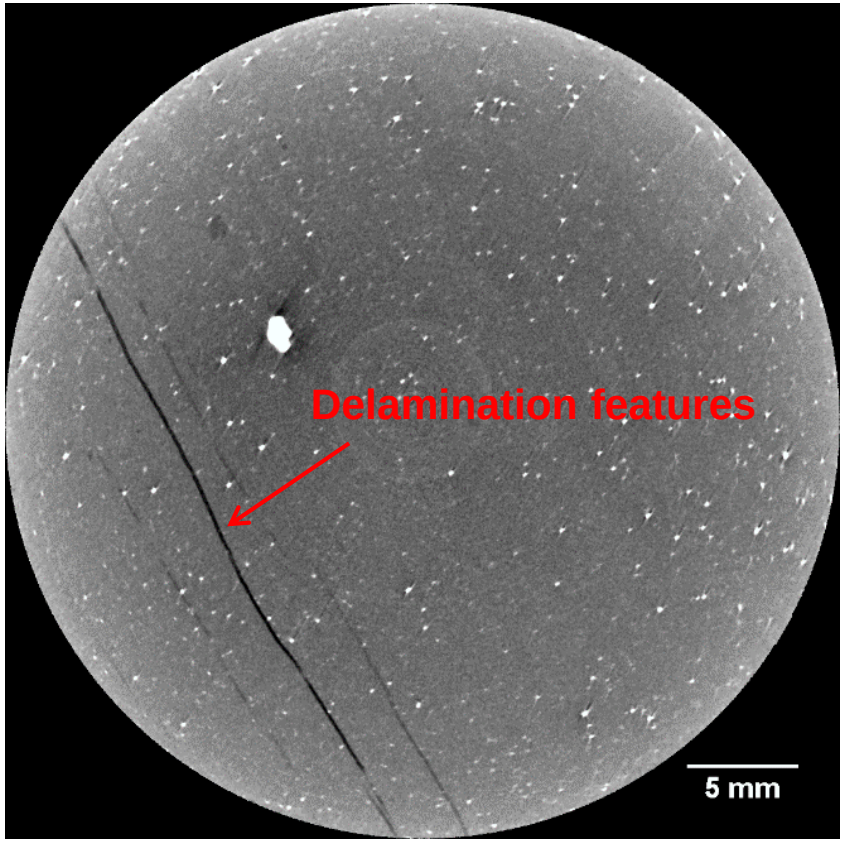

CT image: Marine Shale sample before CO_2 exposure

- Delamination features on Marine Shale sample possibly caused by de-pressurization when retrieving the sample from deep subsurface
- Existence of delamination features may cause over-prediction of permeability increase in CO_2 exposure experiment
- Using a large *n* for permeability calculation in reservoir-scale model is questionable
- Use of small *n* (*n* =1.7) instead of large *n*
- *n* value of 1.7 is validated by previous Selma Chalk caprock work (Zhang et al., under review)

$$\frac{perm_{i,t}}{perm_{i,o}} = \left(\frac{\emptyset_{i,t}}{\emptyset_{i,o}}\right)^{n}$$

Discussion

Extending core-scale results to reservoir scale

Permeability evolution of core sample is not the same as permeability evolution in the field

Core-scale modeling for the host rock: permeability decrease after 180 days of CO_2 exposure

Core-scale modeling for the caprock: permeability increase after 180 days of CO_2 exposure

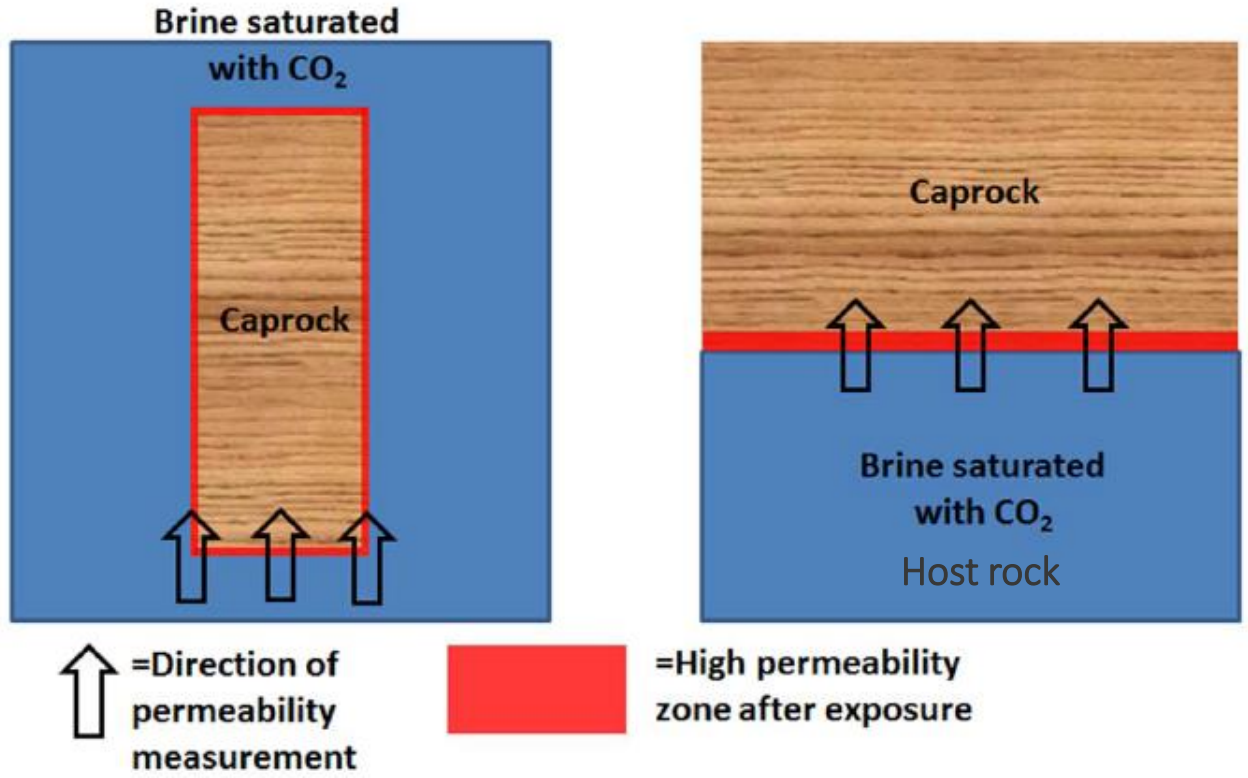

Discussion

Extending core-scale results to reservoir scale

- A reservoir-scale model is developed using TOUGHREACT to investigate porosity and permeability change in both LT CO_2 storage reservoir and Marine Shale caprock
- Important modeling parameters from the core-scale model are the basis to develop the field-scale model

Model set-up

System	Series	Stratigraphic Unit	Sub-Units	Hydrology
Tertiary	Miocene	Misc. Miocene Units	Pascagoula Fm.	Freshwater Aquifers
			Hattiesburg Fm.	
			Catahoula Fm.	
	Oligocene	Vicksburg		Saline Reservoir
			Red Bluff Fm.	Minor confining unit
	Eocene	Jackson		Saline Reservoir
		Claiborne		Saline Reservoir
		Wilcox		Saline Reservoir
	Paleocene	Midway Shale		Confining unit
Cretaceous	Upper	Selma Chalk	Navarro Fm.	Confining unit
			Taylor Fm.	
		Eutaw	Austin Fm.	Confining unit
			Eagle Ford Fm.	Saline Reservoir
		Tuscaloosa Group	Upper Tusc.	Minor Reservoir
			Marine Tusc.	Confining unit
			Lower Tusc.	Saline Reservoir
	Lower	Washita-Fredricksburg	Dantzler Fm.	Saline Reservoir
			"Limestone Unit"	

Modeling region

Stratigraphic column at Plant Daniel CO_2 storage site in Jackson County, MS

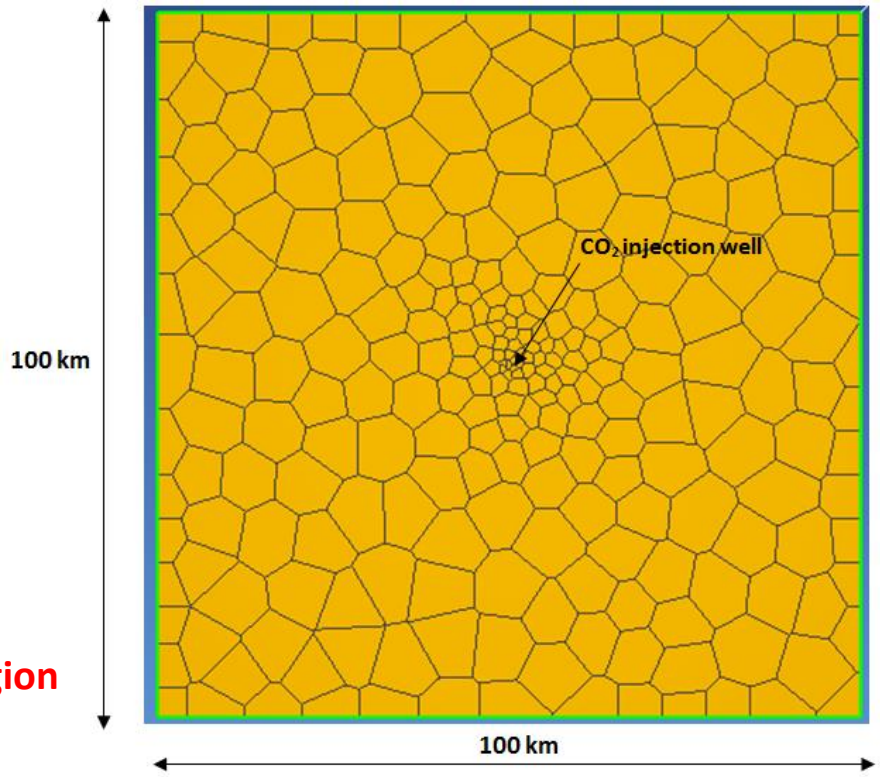

Domain of the reservoir-scale TOUGHREACT model

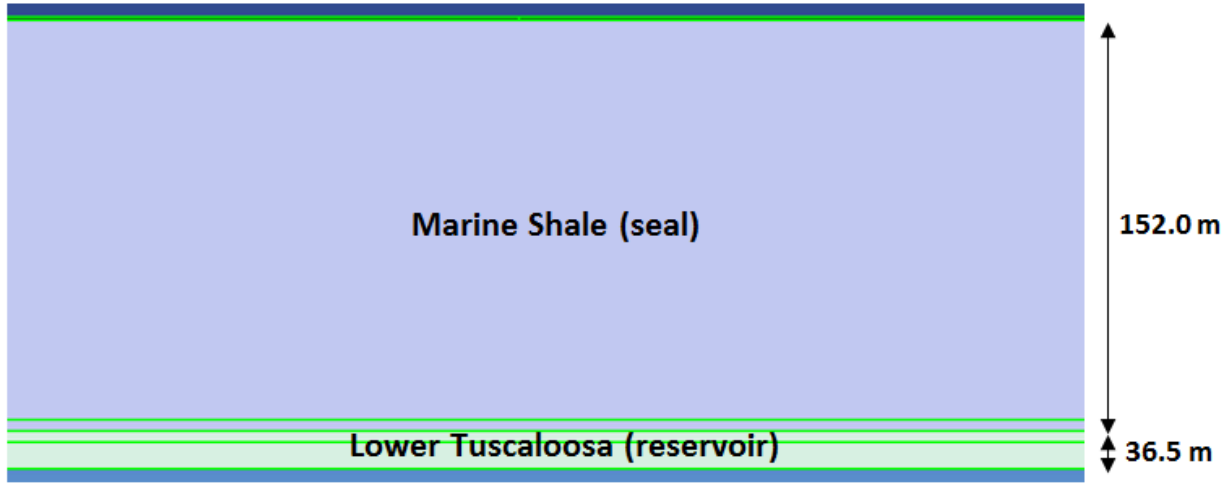

Model set-up

Initial brine concentration and other important modeling parameters

Initial brine concentration

	Synthetic Lower Tuscaloosa Brine, batch # 4
	Ave. (ppm)
Al	1.13
Ba	9.48
Ca	11030
Cr	0.133
Cu	~
Fe	128
K	373
Mg	1009
Mn	~
Na	42063
Ni	0.59
Si	~
Sr	661
Chloride	87524
Bromide	459
Sulfate	235
Initial pH	5.40

Other important modeling parameters

Parameter	Value	Parameter	Value
Density of rock in Layers 1-5	2600 kg/m^3	CO_2 injection rate (constant rate from t=0 to t=30 years)	31.7 kg/s (1MT per year)
Initial pressure at Z=0 m	31.3 MPa	Brine residual saturation	0.20
Pressure gradient	10^4 Pa/m	CO_2 residual saturation	0.05
Temperature at Z=0 m	95 °C	van Genuchten 1/α for capillary pressure calculation	2×10^4 Pa
Temperature gradient	0.025 °C/m	van Genuchten λ for capillary pressure calculation	0.457
Horizontal permeability (storage formation)	2.19×10^{-12} m^2 (2.19 D)	Thickness of the seal	152.0 m
Vertical permeability (storage formation)	2.19×10^{-13} m^2 (0.219 D)	Thickness of the storage reservoir	36.5 m
Horizontal permeability (seal)	4.7×10^{-17} m^2 (4.7×10^{-5} D)	Salt (NaCl) mass fraction in brine	10%
Vertical permeability (seal)	4.7×10^{-18} m^2 (4.7×10^{-6} D)	Porosity (storage formation and formation above the seal)	0.268
CO_2 injection period	30 years	Simulation time step	Automatic adjustment (initial step = 100 s)
Post-CO_2 injection period	100 years	Boundary condition (horizontal)	Open and fixed pressure boundary
Domain size	100 ×100 km	Boundary condition (top and bottom)	No-flow boundary
Maximum brine saturation	0.95	Porosity (seal)	0.0865
Maximum CO_2 saturation	0.80	Rock compressibility	1.2×10^{-10} Pa^{-1}
Maximum simulation time	130 years		

Results and discussion

CO_2 saturation

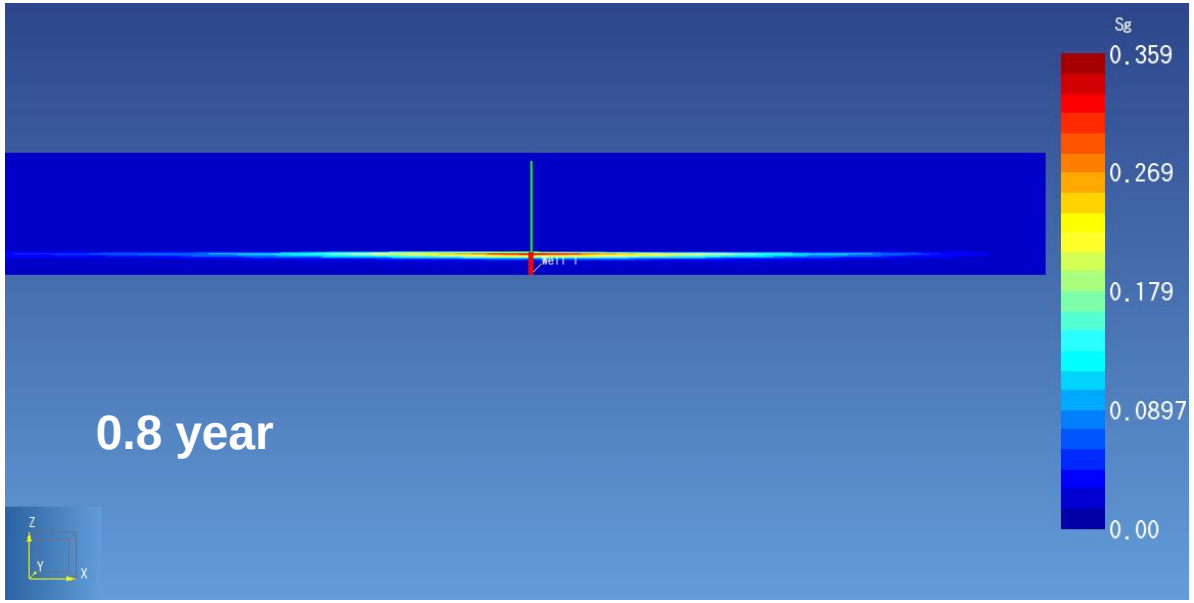

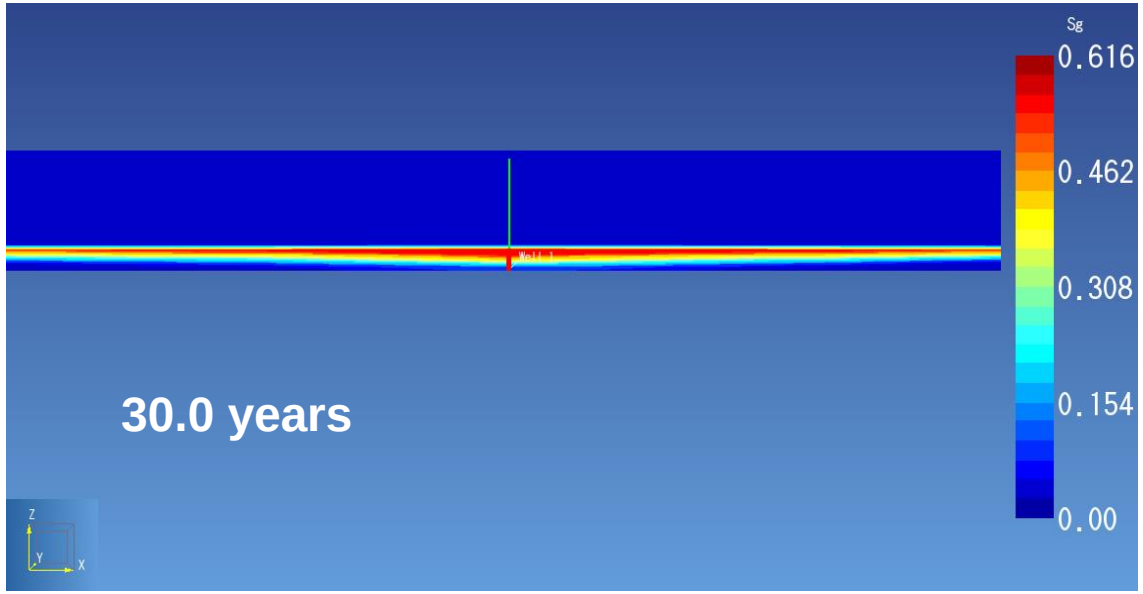

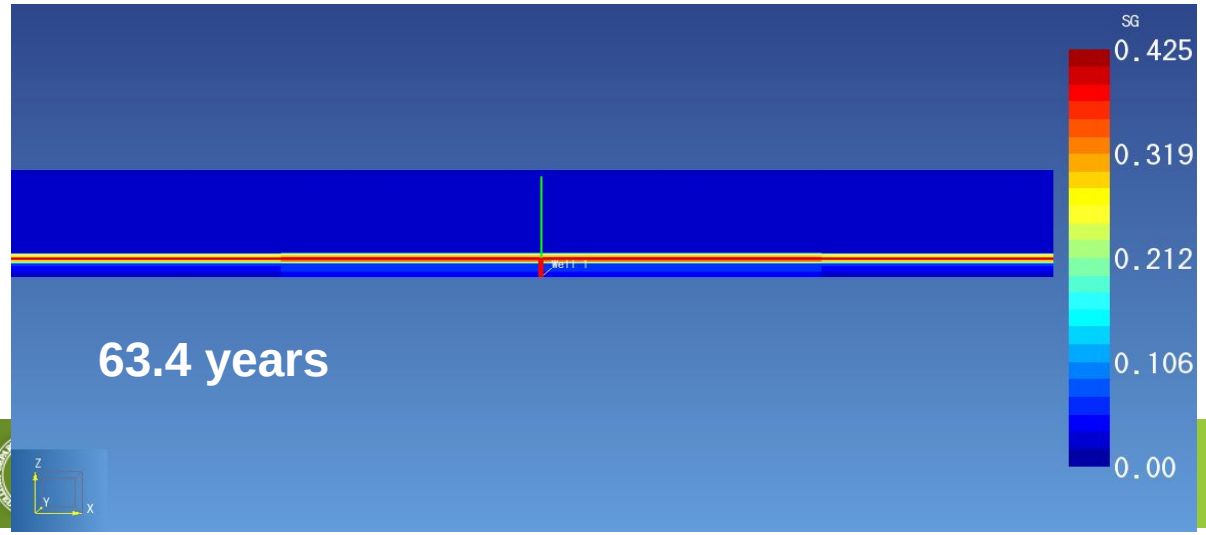

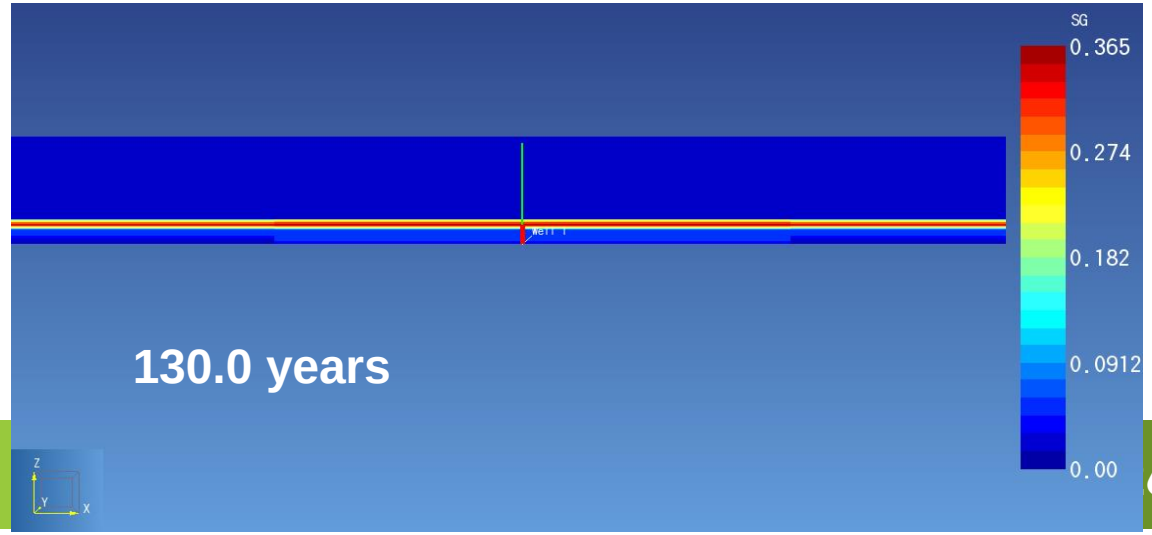

CO_2 saturation—zoom in view

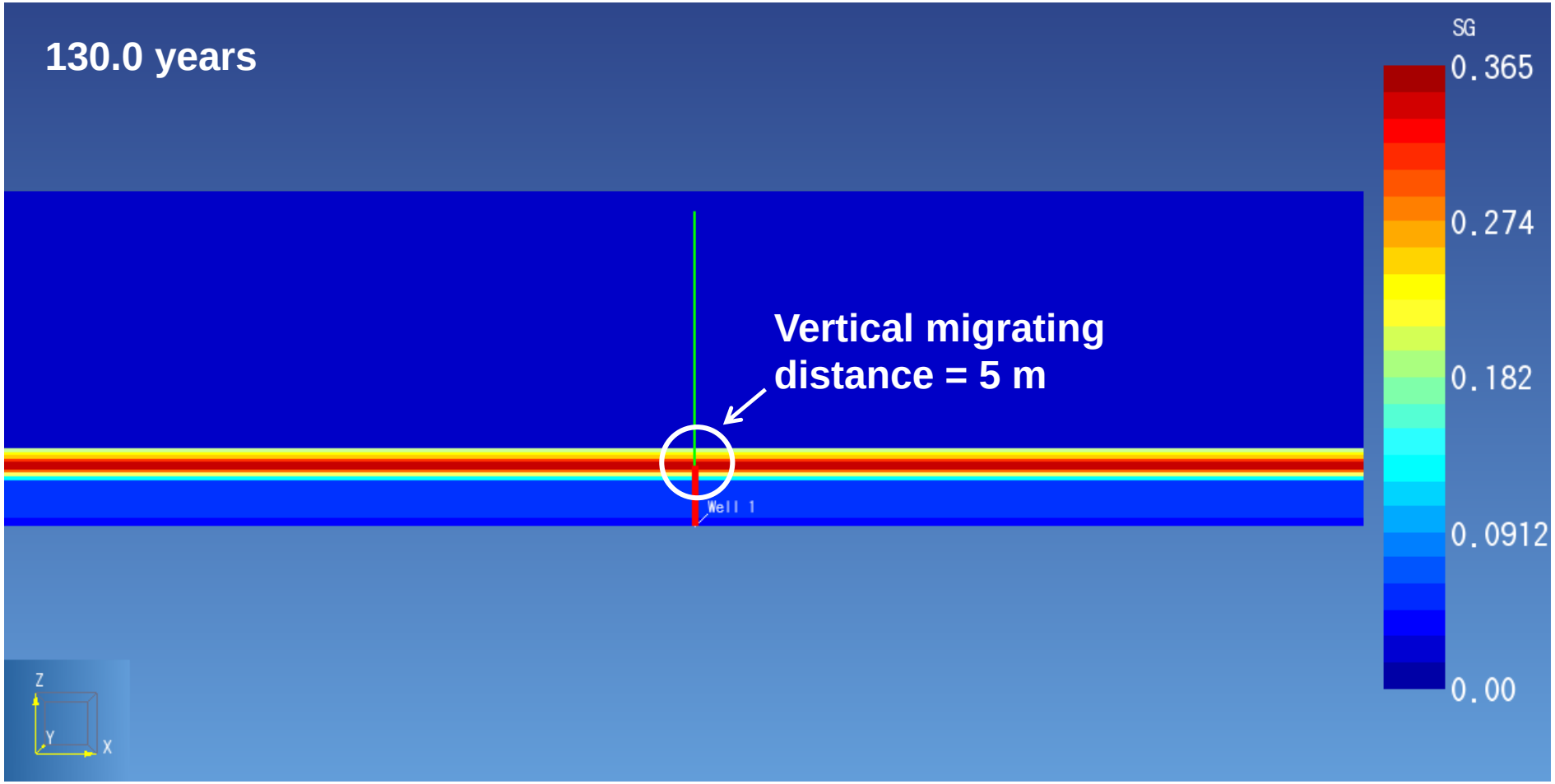

Very slow upward migration of injected CO_2

Results and discussion

pH

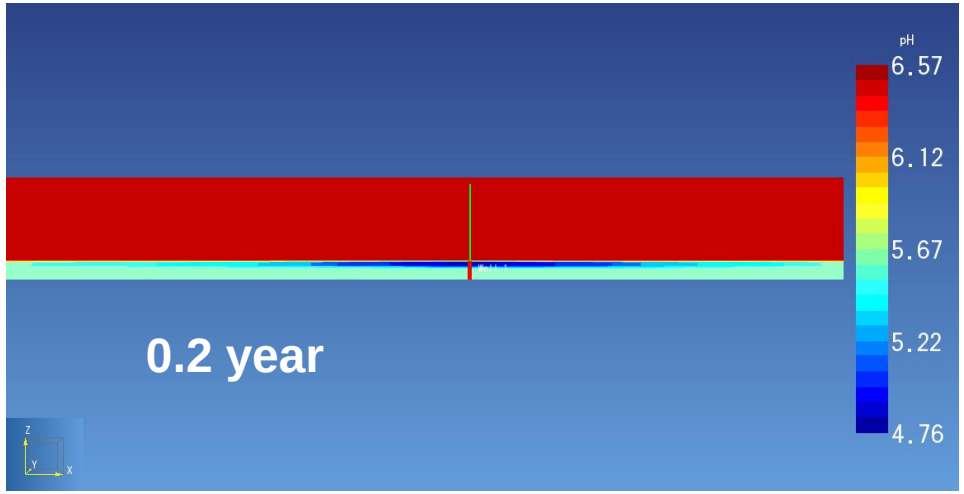

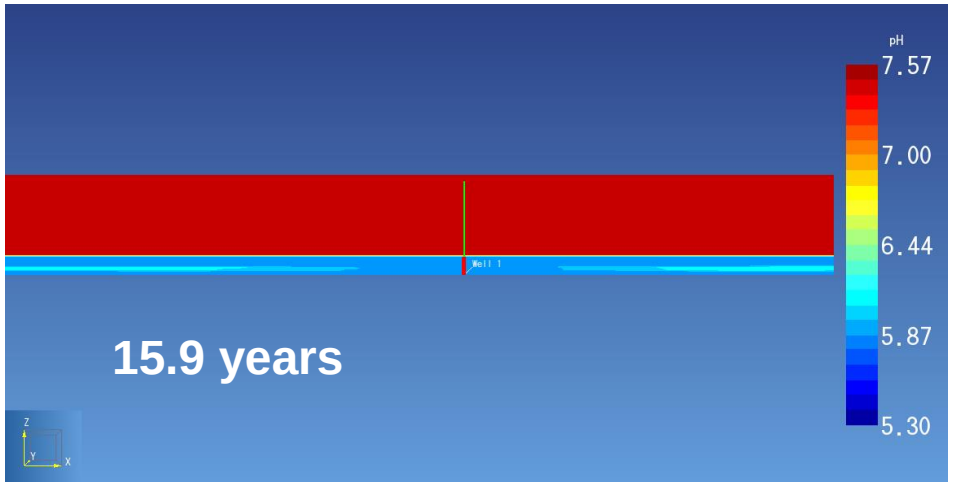

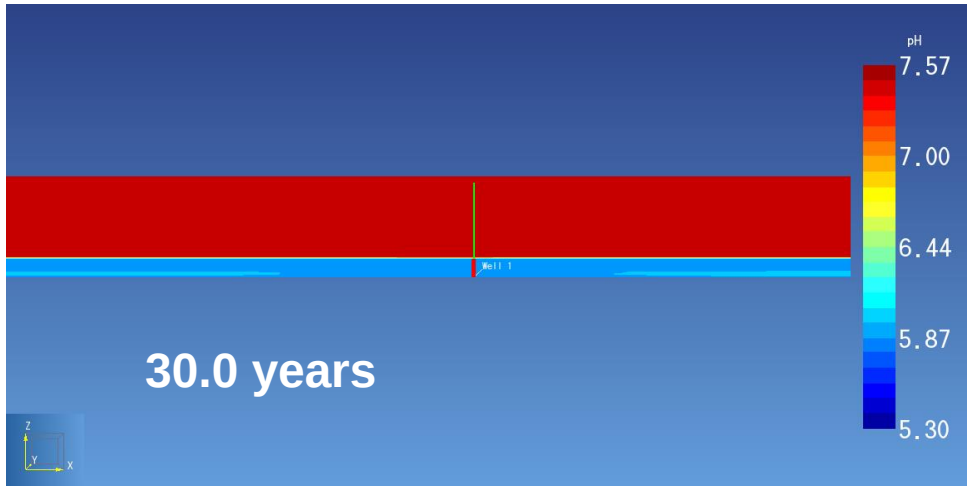

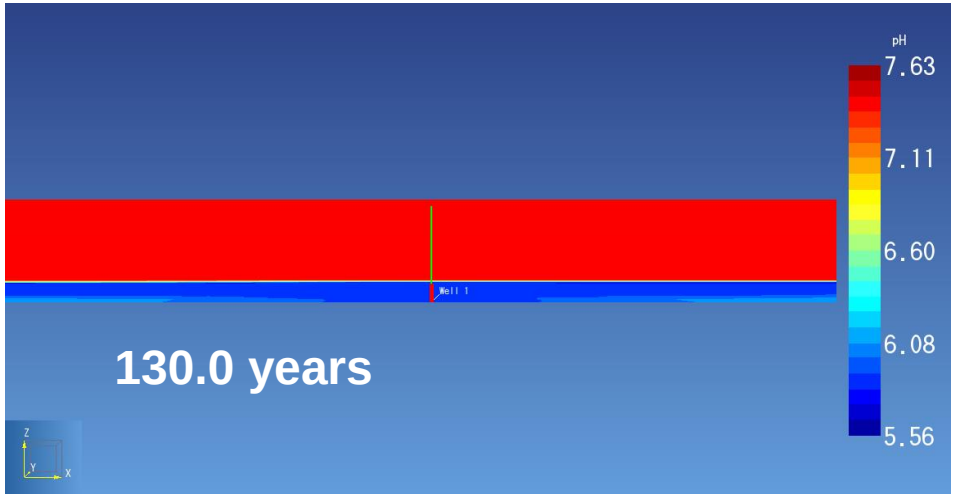

Different from core-scale CO_2 exposure experiment, strong pH buffering effect of the LW Formation in the reservoir-scale simulation significantly rises pH.

Results and discussion

Mineral dissolution

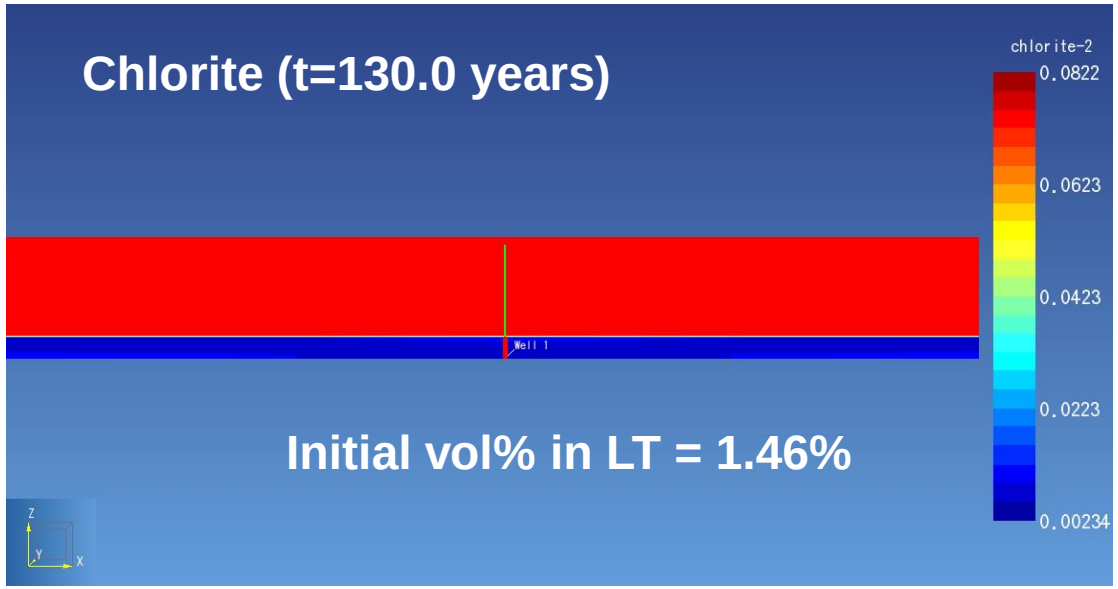

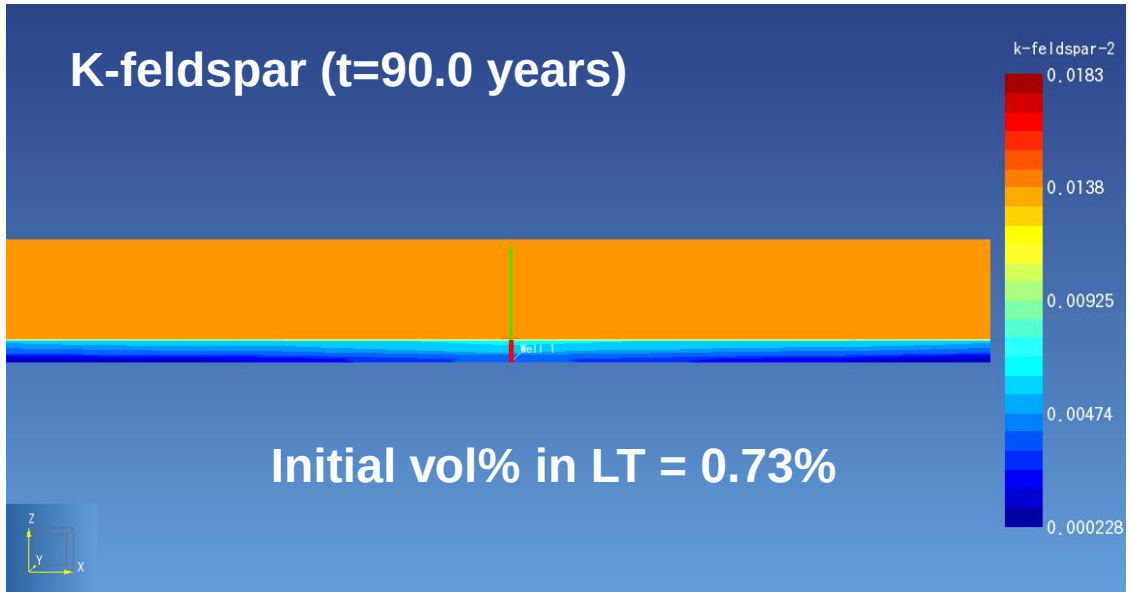

Results and discussion

Mineral dissolution

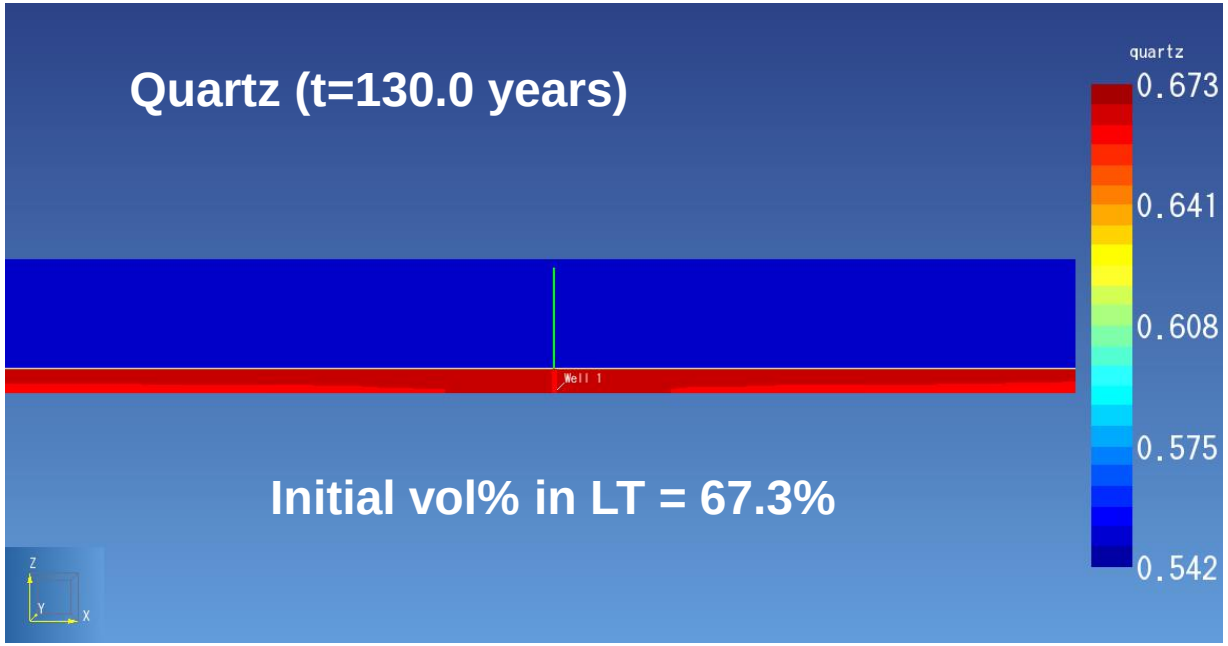

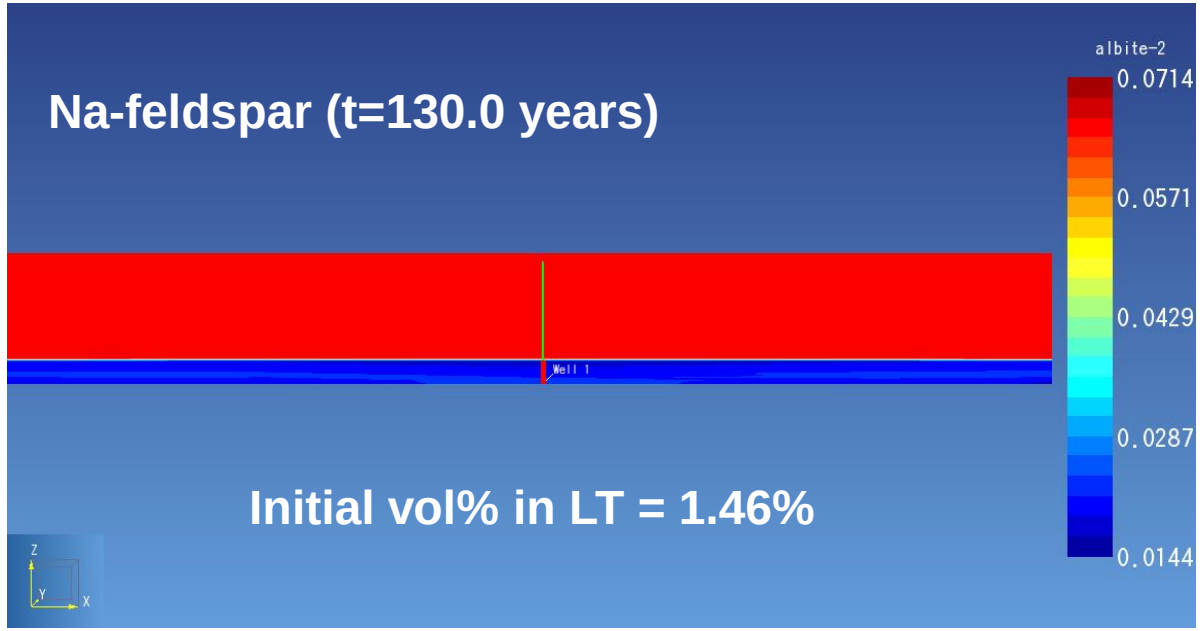

Due to strong pH buffering effect, dissolution of Na-feldspar is not significant.

Results and discussion

Mineral precipitation

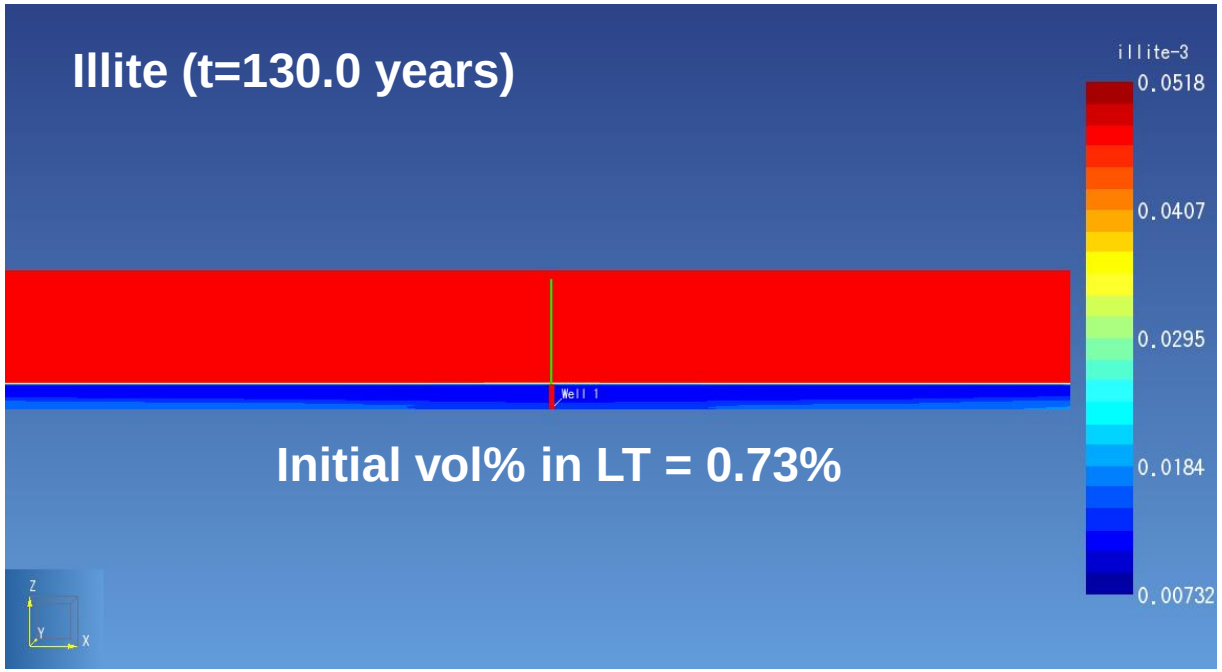

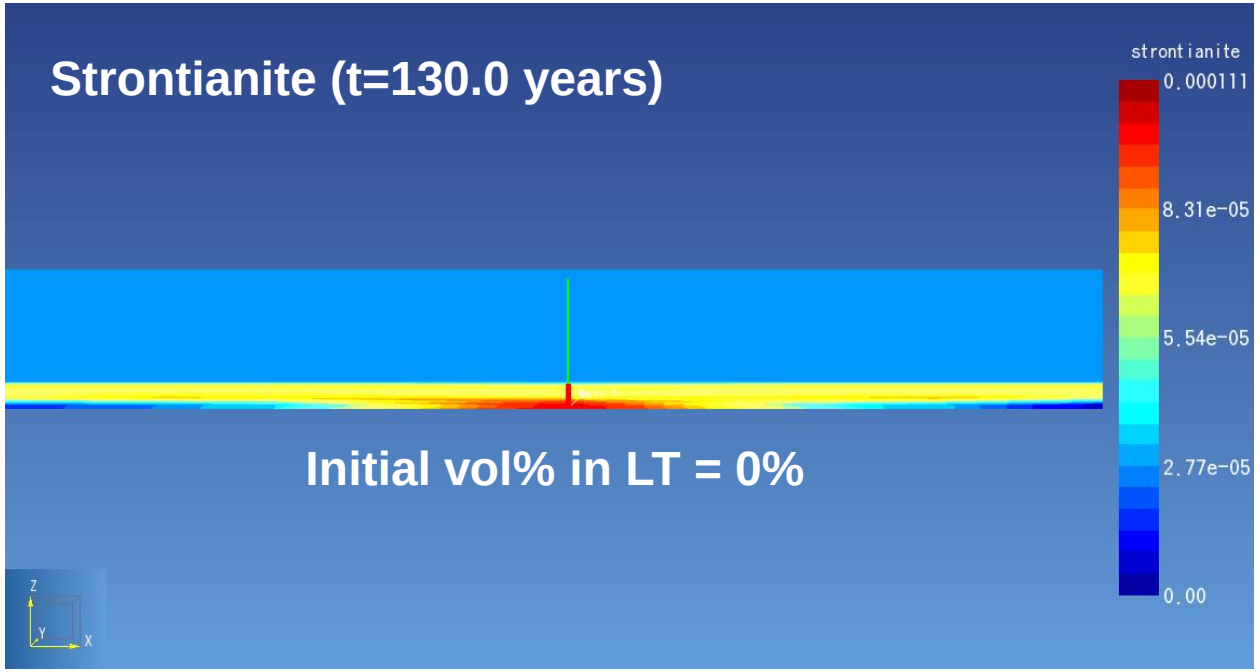

Results and discussion

Mineral precipitation

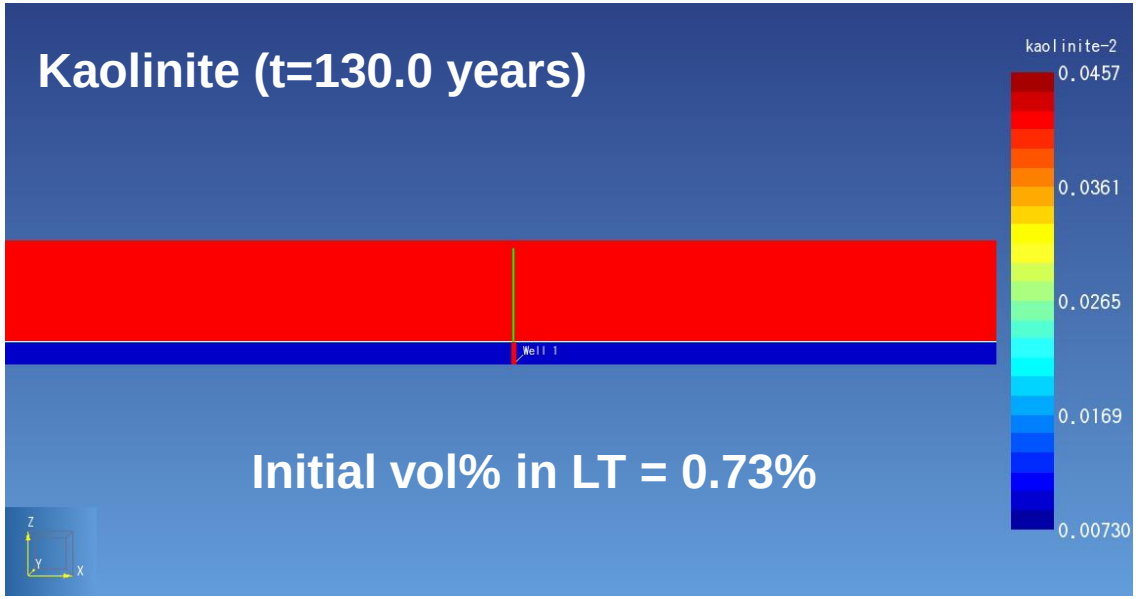

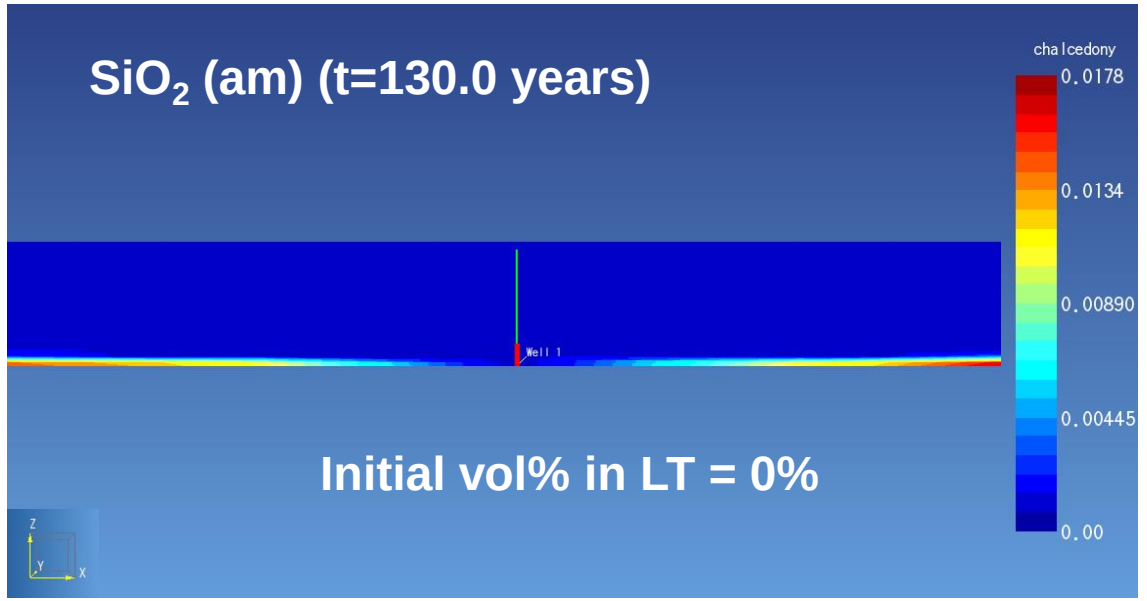

Results and discussion

Mineral precipitation

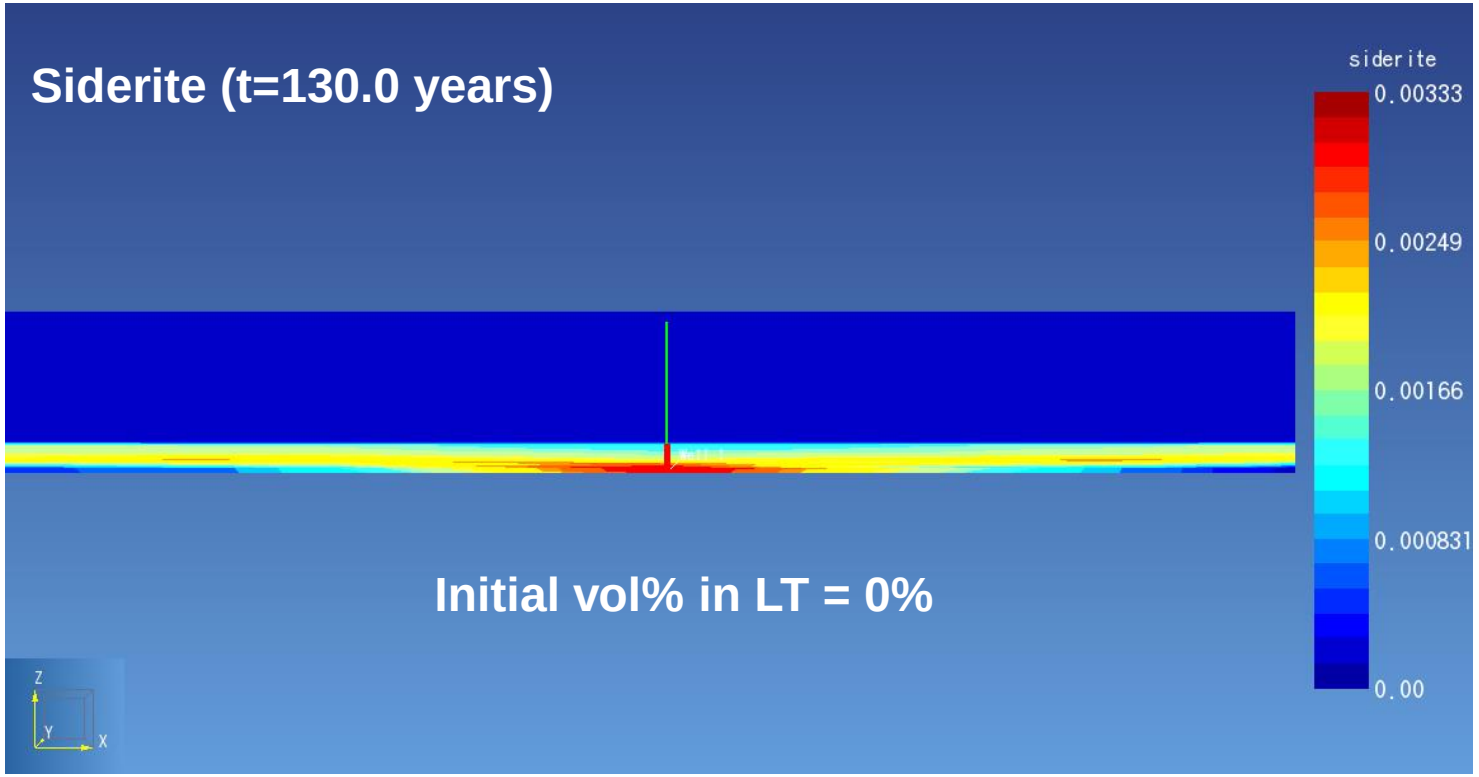

Porosity change

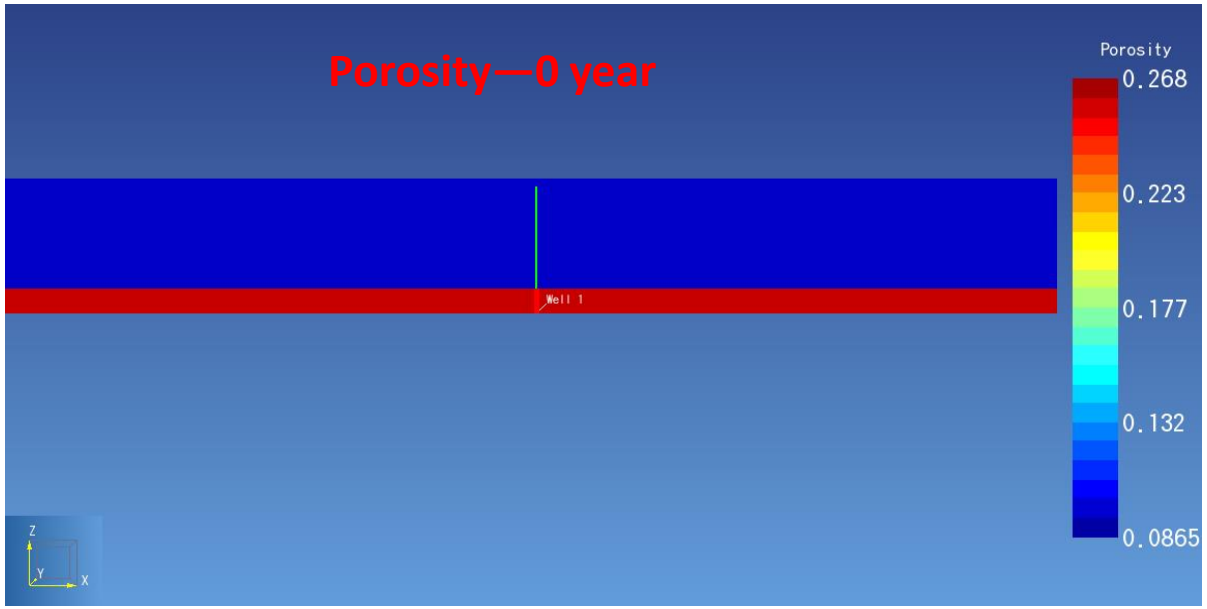

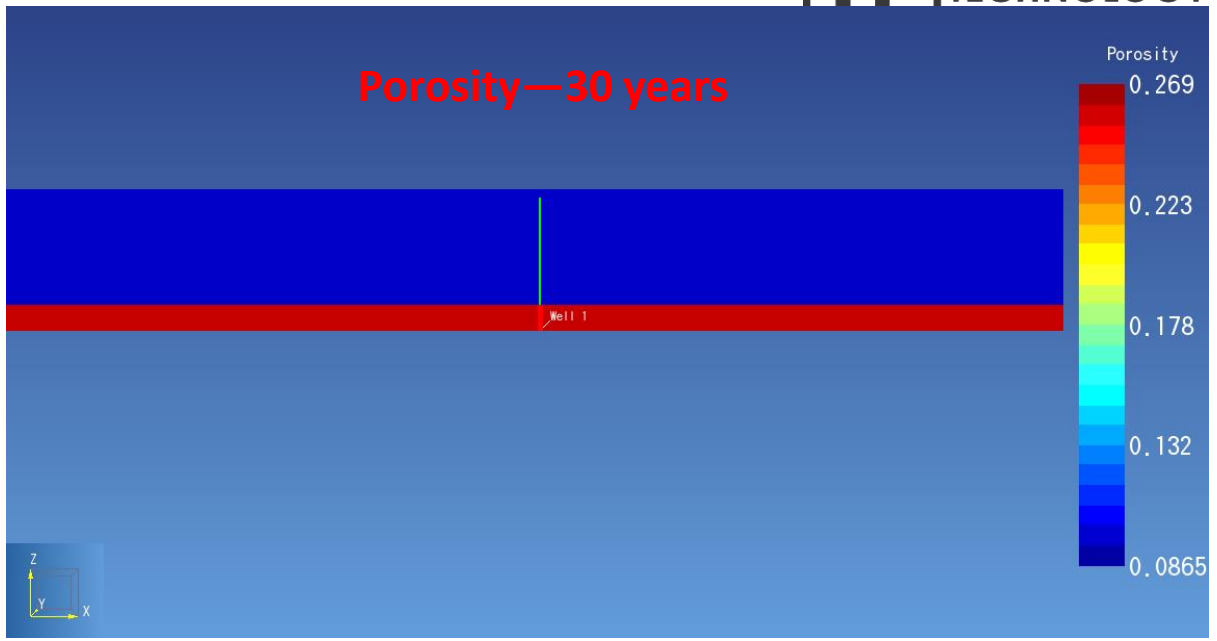

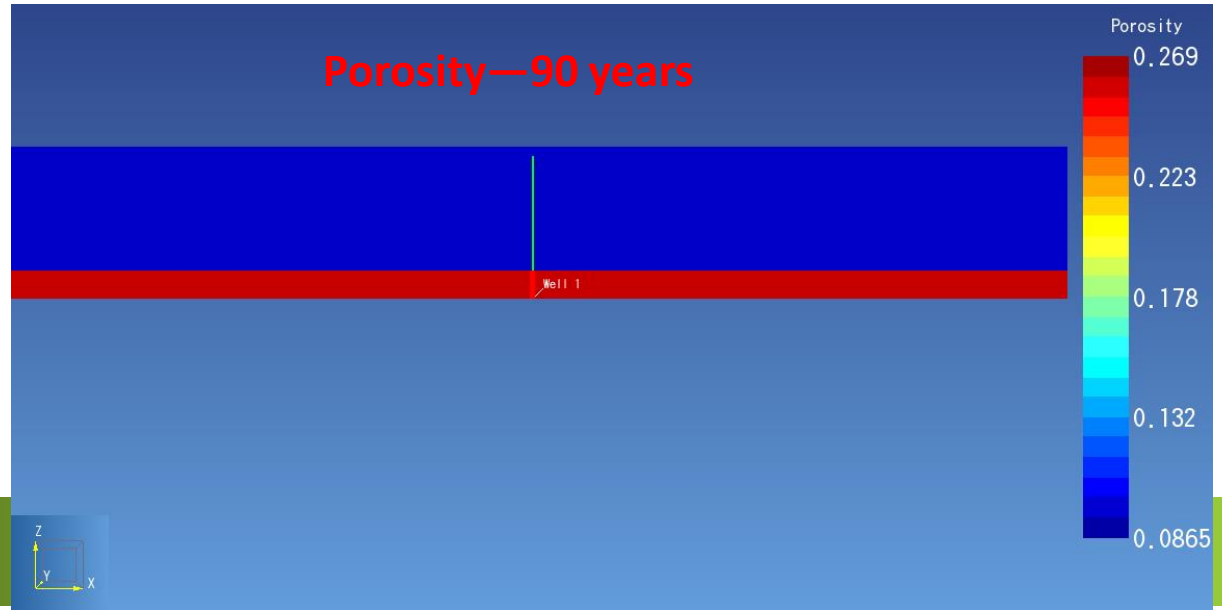

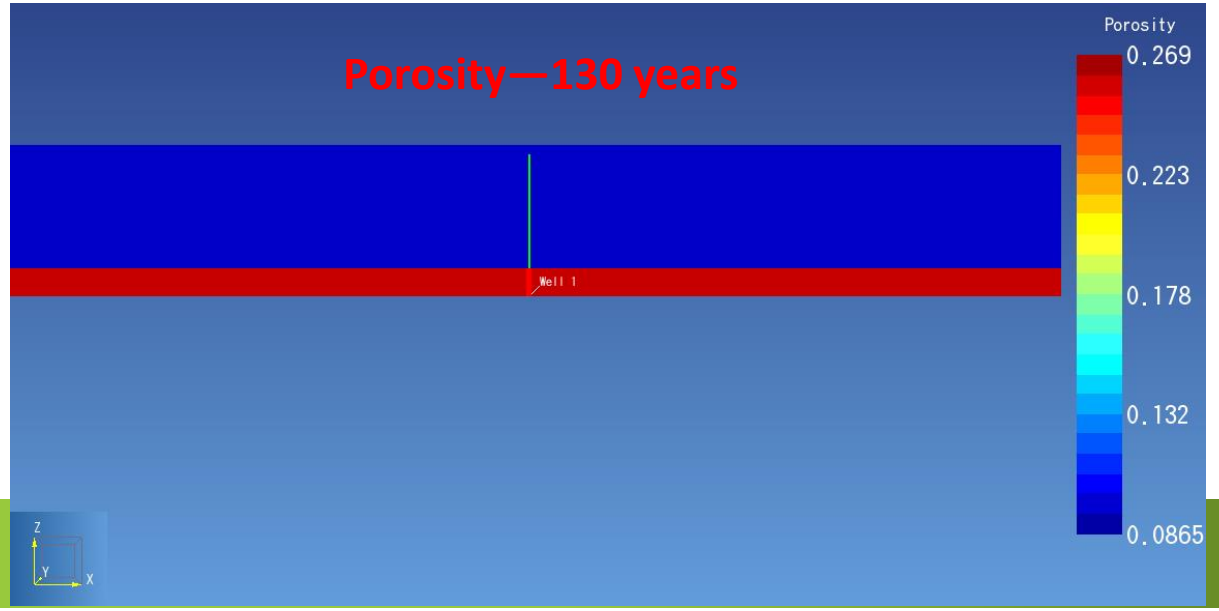

Porosity and permeability change at selected cells (t=130 years)

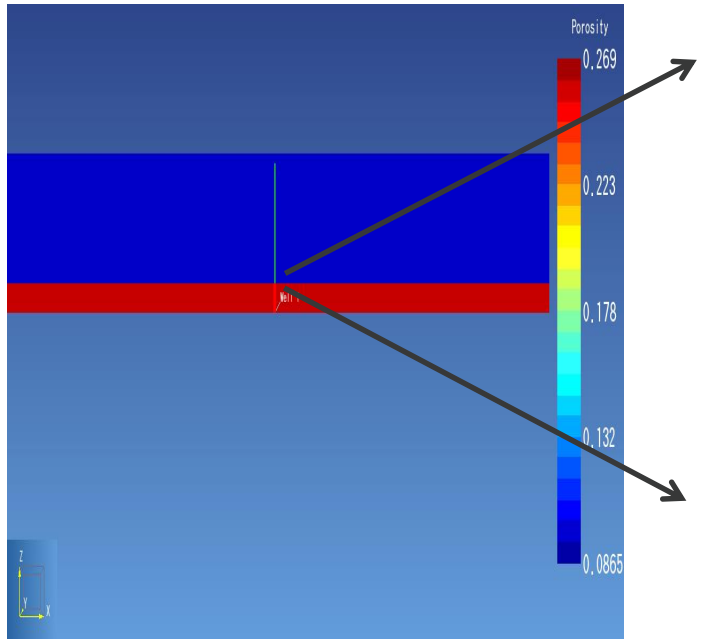

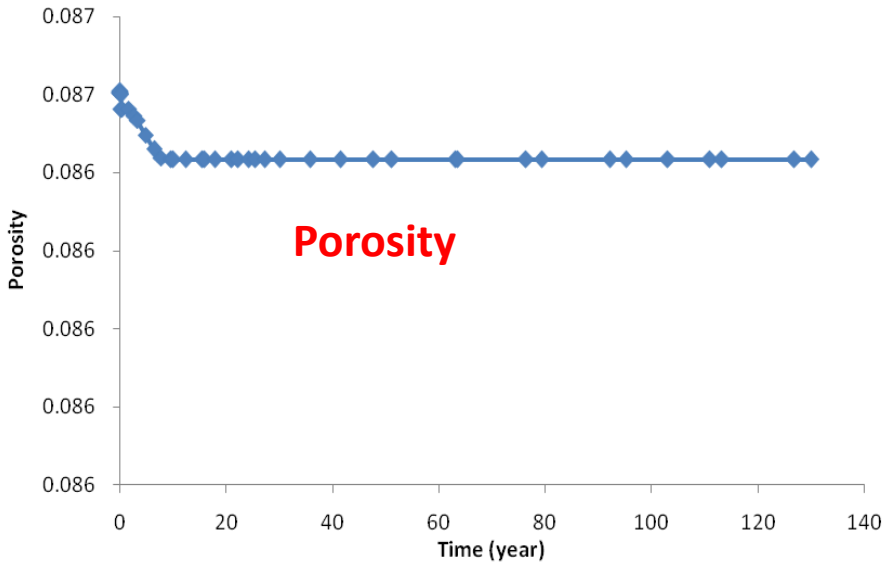

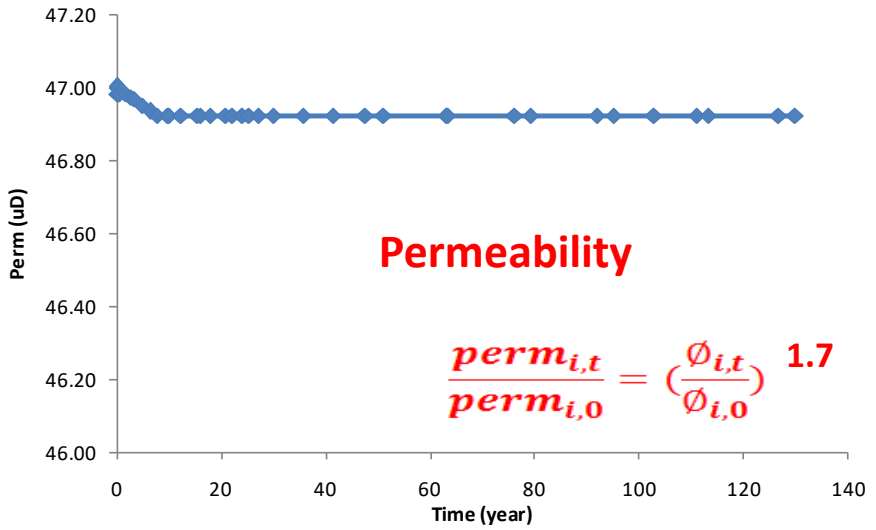

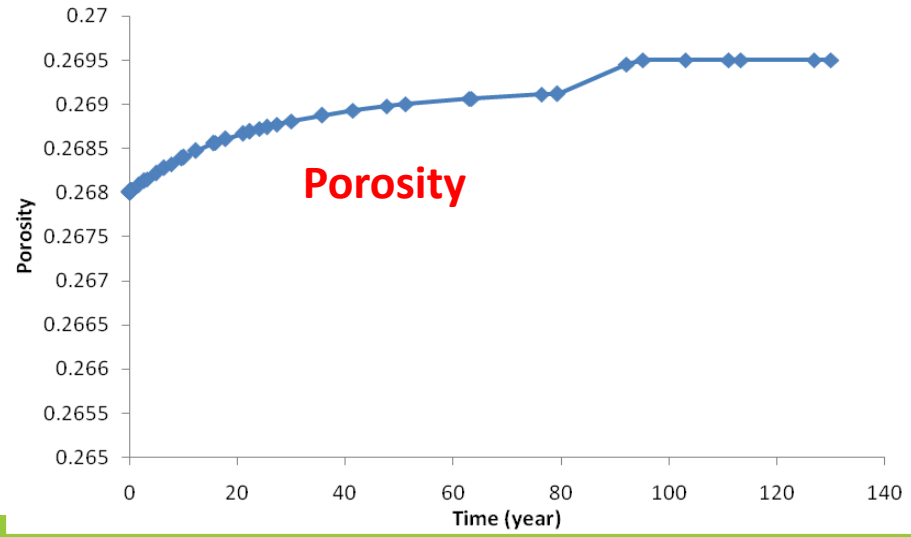

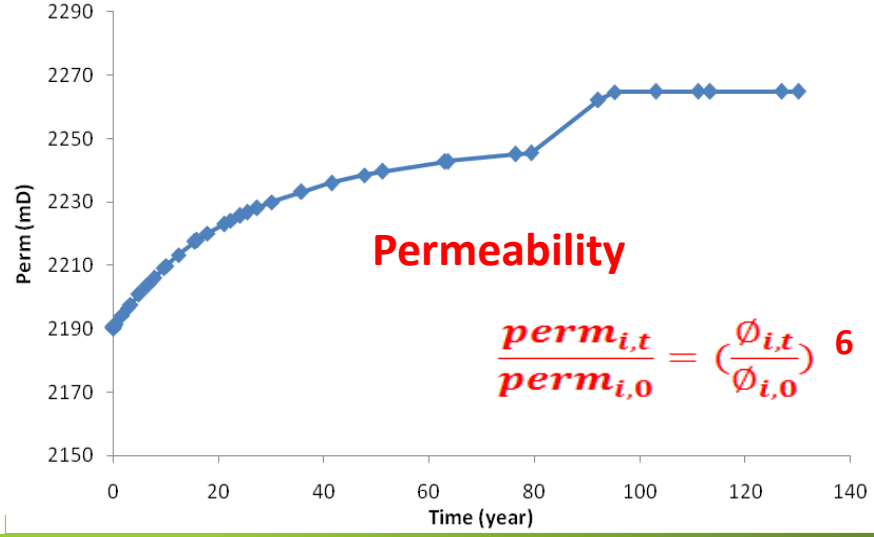

Discussion

- **LW Formation: Porosity increase caused by dissolution of chlorite and K-feldspar; porosity decrease caused by precipitation of SiO_2 (am), siderite and strontianite.**
- **LW Formation: Net porosity increase is small in the 130-year simulation period. Permeability increases from 2190 mD to 2265 mD at a cell close to the injector.**
- **Marine Shale: Negligible porosity and permeability change in the 130-year simulation period.**
- **Strong pH buffering effect is the primary reason to cause small to negligible permeability change of both LW Formation and Marine Shale Caprock.**

Summary

- A reservoir-scale reactive transport model is developed based on modeling parameters validated by CO_2 exposure experiment and core-scale reactive transport model.
- Permeability change predicted by reservoir-scale model is different from permeability change predicted by core-scale model.
- The primary reason to cause discrepancy between reservoir-scale modeling results and core-scale modeling results is the strong pH buffering effect on pore water in LT Formation.
- Mineral dissolution and precipitation have small to negligible impact on porosity and permeability of both LW CO_2 Storage Formation and Marine Shale Caprock in a 130-year period.

NATIONAL ENERGY TECHNOLOGY LABORATORY